Provenance and thermal history of the Beetaloo Basin using Illite crystallinity and zircon geochronology and trace element data.

Thesis submitted in accordance with the requirements of the University of Adelaide for an Honours Degree in Geology

Nicholas Capogreco

November 2017

PROVENANCE AND THERMAL HISTORY OF THE BEETALOO BASIN USING ILLITE CRYSTALLINITY AND ZIRCON GEOCHRONOLOGY AND TRACE ELEMENT DATA.

ABSTRACT

The Beetaloo Basin of the 'greater McArthur Basin', is a 15,000km^2 Palaeoproterozoic depocentre which hosts shallow water, dominantly marine, clastic sedimentary rocks and is a large hydrocarbon reserve. Here I present LA-ICP-MS detrital zircon U-Pb age data, Rare Earth Elemental zircon and illite crystallinity XRD results and compare with existing studies to explore the variation in provenance throughout the basin and to better understand its temperature history as much of the basins history is still unknown. Nine sandstone and seventeen shale core samples were analysed.
New constraints were placed on the depositional age for the Corcoran formation to between 1390 ± 27 Ma and 1324 ± 4 Ma. The Velkerri Formation, Moroak Sandstone and Kyalla Formation of the Maiwok Sub-group all largely supported the results of previous studies yielding comparable maximum depositional ages. Zircon phosphorous concentrations revealed a largely I-type granitic source rock indicating the granites were formed in arc related settings.
Detrital zircon age data revealed possible origins of sediments showing that the Corcoran Formation has a major source of ca. 1600 Ma zircons which are not unlike rocks from Eastern Queensland orogens. The Velkerri Formations main age peak falls at ca. 1765 Ma which shows a change to older detrital source rocks with more similarities to the Arunta and Kathleen and Western Orogenies. Moving up-section to the Moroak Sandstone and Kyalla Formations, samples shift to younger ca. 1560 Ma peak ages at the base of the Moroak followed by a gradual increase in age with younger sequences where a maximum peak age of ca. 1795 Ma is found in the mid Kyalla Formation. This gradual increase shows a gradual shift in sediment source from e/se sources to southern source regions. Illite crystallinity data shows that the shales within the Beetaloo Basin have experienced much greater temperatures than at present. Altree 2 has an XRD calculated bottom-hole temperature of 155°C at 1647m depth, the Jamison records 156°C at 1695m with the Elliot being the hottest at 194°C at 1697 deep. These values were then used to calculate the amount of cover removed from present day. Altree 2 returned an estimate of 2050m of cover removed, Jamison 1769m and Elliot with the most cover removed at 2680m showing that the southern region of the Beetaloo Basin has experienced the greatest uplift since maximum subsidence followed by the northern Altree 2.

KEYWORDS

McArthur Basin, Beetaloo Basin, Maiwok, Roper Group, Detrital, Zircon Geochronology, Provenance, illite.

CONTENTS

LIST OF FIGURES AND TABLES

INTRODUCTION

The Greater McArthur Basin is a vast and relatively flat lying 550,000km^2 basin that is mainly located in the Northern Territory of Australia, but also reaches into Western Australia and Queensland (Rawlings, 1999; Jackson et al., 2000; Abbott and Sweet, 2001; Ahmad et al., 2013; Betts et al., 2015 Munson, 2016). It hosts sedimentary rocks that date from the Palaeoproterozoic to Neoproterozoic. The processes that led to the formation of the McArthur Basin are still not completely understood as much of the basin is not exposed due to extensive cover and much of the basin knowledge is derived from drill core.

The Wilton Package within the greater McArthur basin is up to 3.5km thick and is comprised mostly of sedimentary rocks with some igneous provinces. The package contains mostly shallow-marine shelf and shoreline deposits (Munson 2016) which are distributed over the 145,000km^2. These deposits are hosted in the McArthur Basin and the Beetaloo Basin, the Tomkinson Province, the Birrindudu Basin and likely in the South Nicholson basin to the south east. The Roper Group of the McArthur Basin, a sub group of the Wilton Package, is dominated by marine siliclastic sedimentary rocks in a series of alternating cross bedded sandstone and shale successions (Jackson et al, 1988; Abbott and Sweet, 2001).

The uppermost part of the Roper group is the main focus of this project. This is called the Maiwok Sub-group. This sub-group is distinguished by a greater proportion of finer shale units than the sandstones below in the Collara Sub-group (Abbot et al., 2001). It hosts shales high in organic carbon in the Velkerri Formation (Cox et al., 2016) and is of great commercial interest as an unconventional petroleum and shale gas producer

(Close et al, 2017; Revie, 2017). The Beetaloo Sub-basin spans approximately 15,000km^2 and is interpreted as being the depocentre of the Roper Group as it holds the thickest stratigraphic units (>3,500m) and is linked to the surrounding basins (Fig. 1). The aim of this research is to build and expand on previous geochronological data undertaken in the Beetaloo Basin. Nine sandstone samples and seventeen shale rich samples have been taken from the Altree 2, Jamison and Elliot wells from within the Beetaloo Basin and cover an 80km north-south transect. Multiple formations (Corcoran formation, Lower Velkerri, Upper Velkerri, Moroak Sandstone, Kyalla and Bukalara) have been targeted. Detrital zircon U-Pb and rare earth elemental (REE) analysis have been used for provenance history and intra basin correlations and were completed using laser ablation inductively coupled plasma mass spectrometry (LA-ICP-MS). The zircon analyses will help determine whether the basin has received sediment from multiple sources or a single source and will aid in constraining depositional ages of formations. Illite crystallinity data have been used for low temperature thermometry across the basin and was analysed via x-ray diffraction (XRD). This thermal analysis will be used to determine whether the Beetaloo Basin has experienced more subsidence in the past or is at its maximum depth today through temperature correlations.

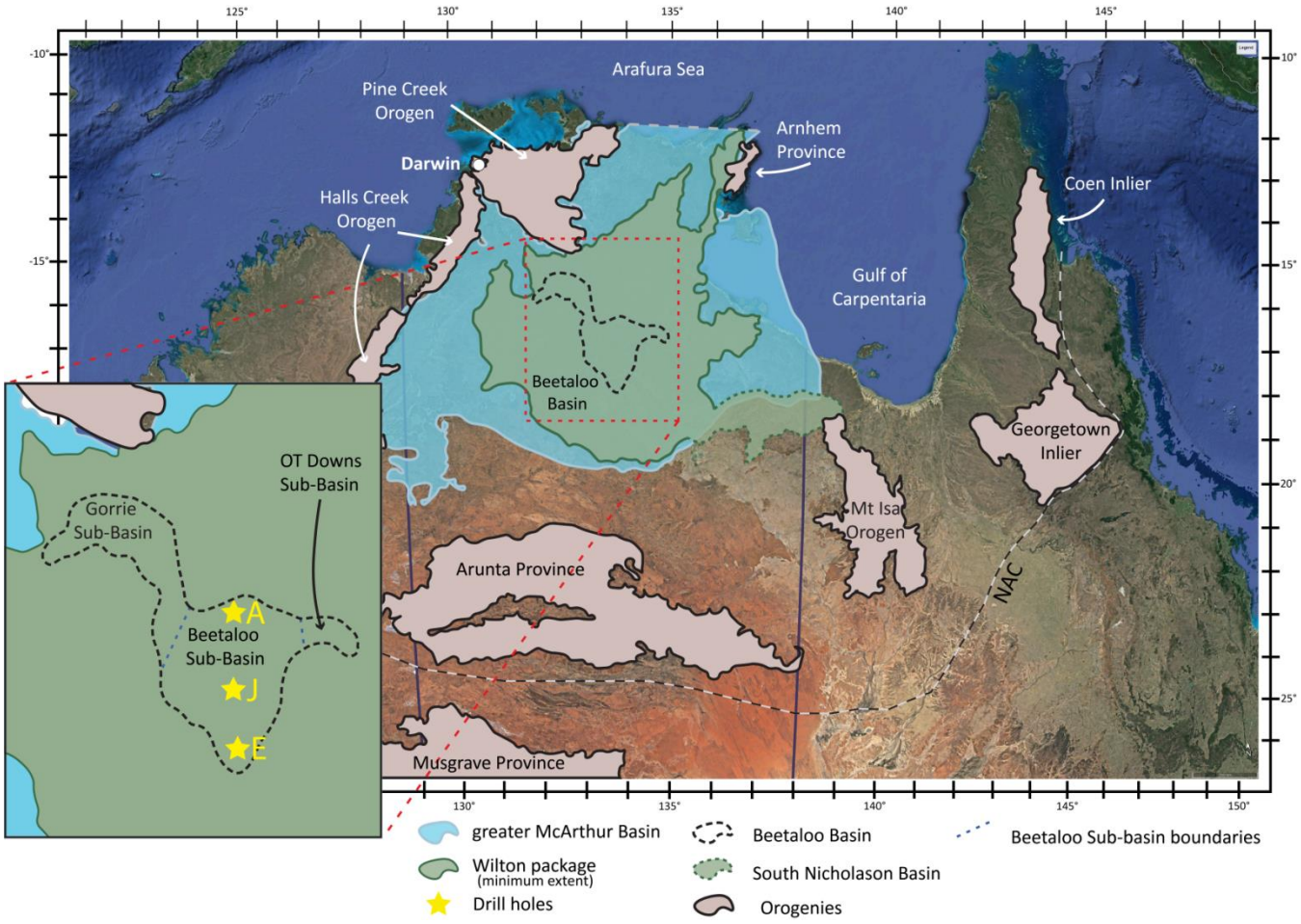

Figure 1: Location map of the study area within the North Australia Craton (NAC). The map shows the location of the Beetaloo Basin within the greater McArthur Basin and surrounding orogens proposed to be basin sediment source. Inset shows the sub basins of the Beetaloo Basin and the location of the drill holes in this study. A = Altree 2, J = Jamison 1 and E = Elliot 1.

GEOLOGICAL SETTING/BACKGROUND

A stratigraphic log is provided in **Figure 3**.

The Roper Group consists of shallow marine siliclastic sediments contained in six regressive-transgressive sequences which have been interpreted as being deposited in a coastal-delataic system (Munson, 2016). These sequences have been grouped into two sub-groups, the Maiwok Sub-group above and the Collara Sub-group below. The Maiwok Sub-group is approximately 2000m thick and distinguished by the abundance

of fine siltstone beds. The Collara Sub-group, which has not been drilled to its maximum depth, is primarily dominated by sandstone with interbedded silt/mudstone and both sub-groups have been interpreted as being deposited in shallow marine to shoreface type environment with rare terrestrial sediments (Abbott and Sweet, 2000; Abbott et al., 2001; Munson, 2016). A disconformity separates the two sub-groups and, along with evidence of syn-and post depositional faulting in basin geometry, shows that the basin has experienced tectonic uplift and subsidence throughout its history (Rawlings et al., 2004; Betts et al., 2015). A regional unconformity, interpreted to be the product of to the ca. 1580-1500Ma Isan Orogeny (Jackson, 1999; Ahmad at al., 2013), connects the base of the Roper Group and the Mesoproterozoic Nathan Group below. This unconformity has been used to constrain the maximum age of deposition of the Roper Group.

Formation models and interpretations of sediment source of the Roper group have been proposed although they are not all in agreement with one another. Abbott and Sweet (2000) proposed that the basin subsidence was due to orogenic flexure resulting from crustal loading which has also been used to explain sediment supply for the Roper Group. Betts and Giles (2006), however, proposed that the accommodation is due to an extensional type basin. It is well understood that the Roper Group formed within an epicontinental sea in the North Australian Craton (NAC) analogous to the modern day inland seas such as the Black Sea (Munson, 2016; Revie, 2017). Sediment sources for the Roper Group potentially lie in multiple surrounding orogenies. Some of these are shown in Fig. 1 and include the Pine Creek Orogen to the north, the Arnhem Province to the northeast, the Halls Creek Orogen to the west, the Arunta Region and Musgrave

Province in the south, the Mount Isa Province to the east and Coen and Georgetown Regions in the far-east.

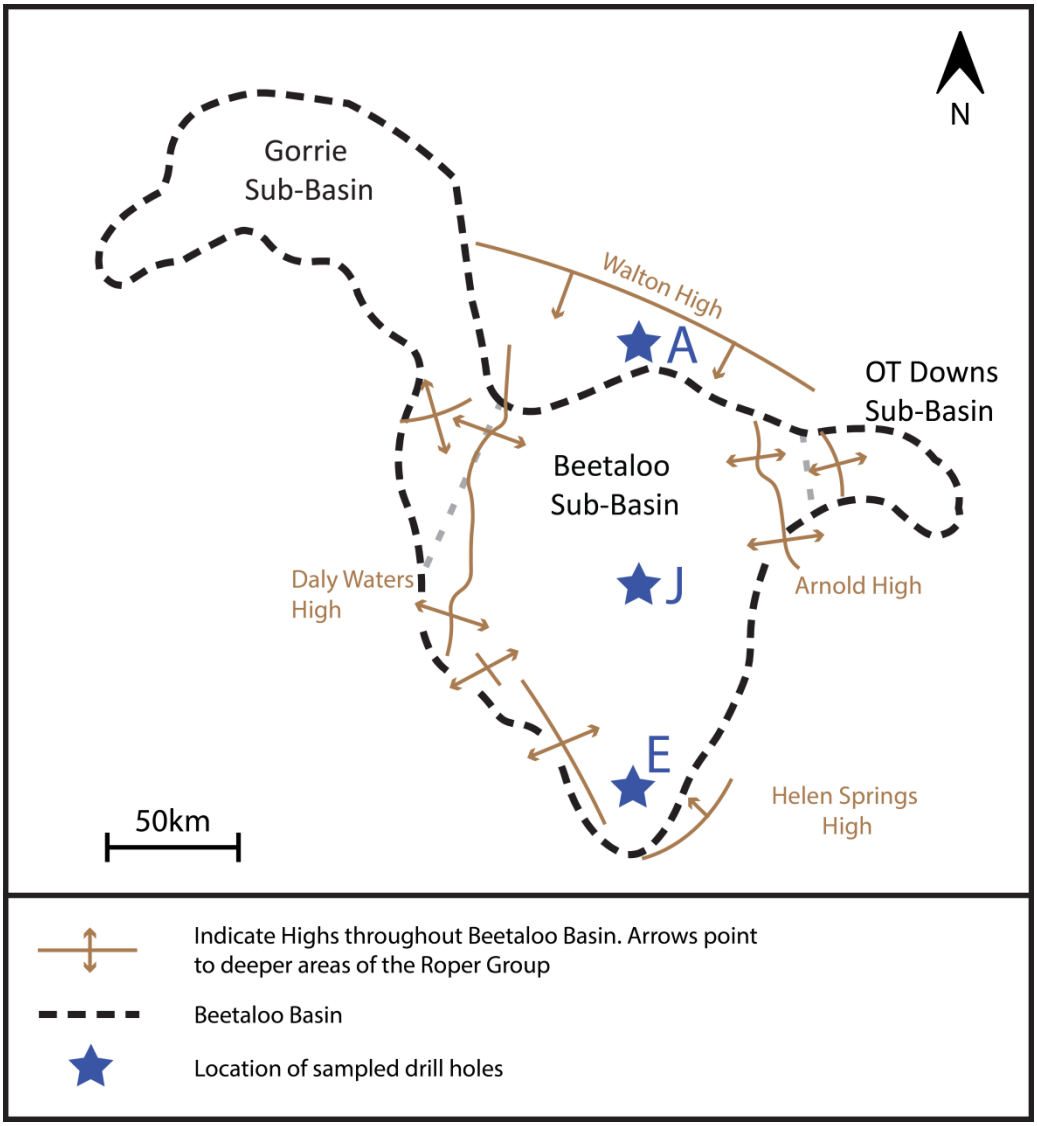

Figure 2: Simplified diagram of the Beetaloo Basin highlighting tectonic elements, basin extent and the location of drill holes from this study. Location of basin highs from Betts et al. (2015).

The Beetaloo Basin, as used in this contribution, consists of multiple smaller sub-basins (Fig. 2) which are the Gorrie Sub-basin in the west which is separated from the Beetaloo Sub-basin in the centre by the Daly Waters High and the OT Downs Sub-basin to the east which is separated by the Arnold High. Faulting north of the Beetaloo Basin comes in the form of the Mallapunyah Fault Zone and Lagoon Creek Fault Zone with

the wide Batten Fault Zone to the west. The extent of the Beetaloo Basin is constrained by the east-west trending Walton High in the north and the NE-SW trending Helen Springs High in the south. These highs, particularly the Walton High, have been seen to differentiate U-Pb spectra suggesting they were present during the time of sediment deposition (Yang et al., in review).

Within the Beetaloo Basin the Maiwok Sub-group contains 5 formations, each has been categorised based on its lithology and placed into two main groups, coarser grained sandstones or fine grained mud/siltstones. The sandstone dominated units are characterised as being fine to medium grained quartz rich sediments and consist of (in order of oldest to youngest) the Bessie Creek Sandstone and Moroak Sandstone. The shale and mudstone dominated units host finely laminated siltstone and mudstones with some sandstone cross bedding and are the Corcoran Formation, Velkerri Formation and Kyalla Formation, the latter of the two hosting potential resources for unconventional petroleum and shale gas (Close et al., 2016; Revie, 2016).

The Urpapunga Region (Fig. 1) is intruded by the Derim-Derim Dolerite, dated at 1324 ±4Ma (Abbott et al., 2001). This dolerite sill intrudes all formations in the Maiwok Sub-group in this region, except for the Chambers River formation, and can be used as a constraint on the minimum depositional age (Abbott et al., 2001). The unconformity between the Roper Group and the Nathan Group can also be used to constrain maximum depositional age to between ca. 1580 and ca.1500Ma (Jackson et al., 1999).

METHODS

Zircon Preparation

For zircon analysis, nine sandstone samples were collected from the Northern Territory Core store and selected for the cleanest sandstone formations. Table 1 below lists the locations of all sandstone samples taken.

Table 1: List of all samples taken from drill core for zircon analysis

Well	Sample Name	Formation	Depth (m)
Altree 2	AN2	Upper Velkerri	573.0
	AN3	Lower Velkerri	1128.9
	ALT09	Corcoran Formation	1670.0
Jamison	JN1	Bukalara Formation	481.1
	JN5	Kyalla Formation	1278.4
	JN6	Kyalla Formation	1587.0
Elliot	EN4	Kyalla Formation	1021.5
	EN8	Moroak Sandstone	1367.3
	E18	Moroak Sandstone	1697.4

To extract zircons, core samples were milled until medium grain sized sand was achieved and sieved to retain 79um to 400um grain size fractions. Zircons were separated from the bulk sample via panning and traditional magnetic and heavy liquid methods. To reduce the effect of bias, zircons of all colours, shapes and size were hand-picked under a binocular reflected-light microscope. Grains were mounted onto epoxy slides, polished and carbon coated. Zircon grains were imaged through Cathode luminescence on a Gatan CL detector (working distance: 15mm; accelerating voltage: 12kv) attached to a Quanta 600 Scanning Electron Microscope (SEM) at Adelaide Microscopy to determine ideal spot site for U-Pb and rare earth element laser analysis (REE).

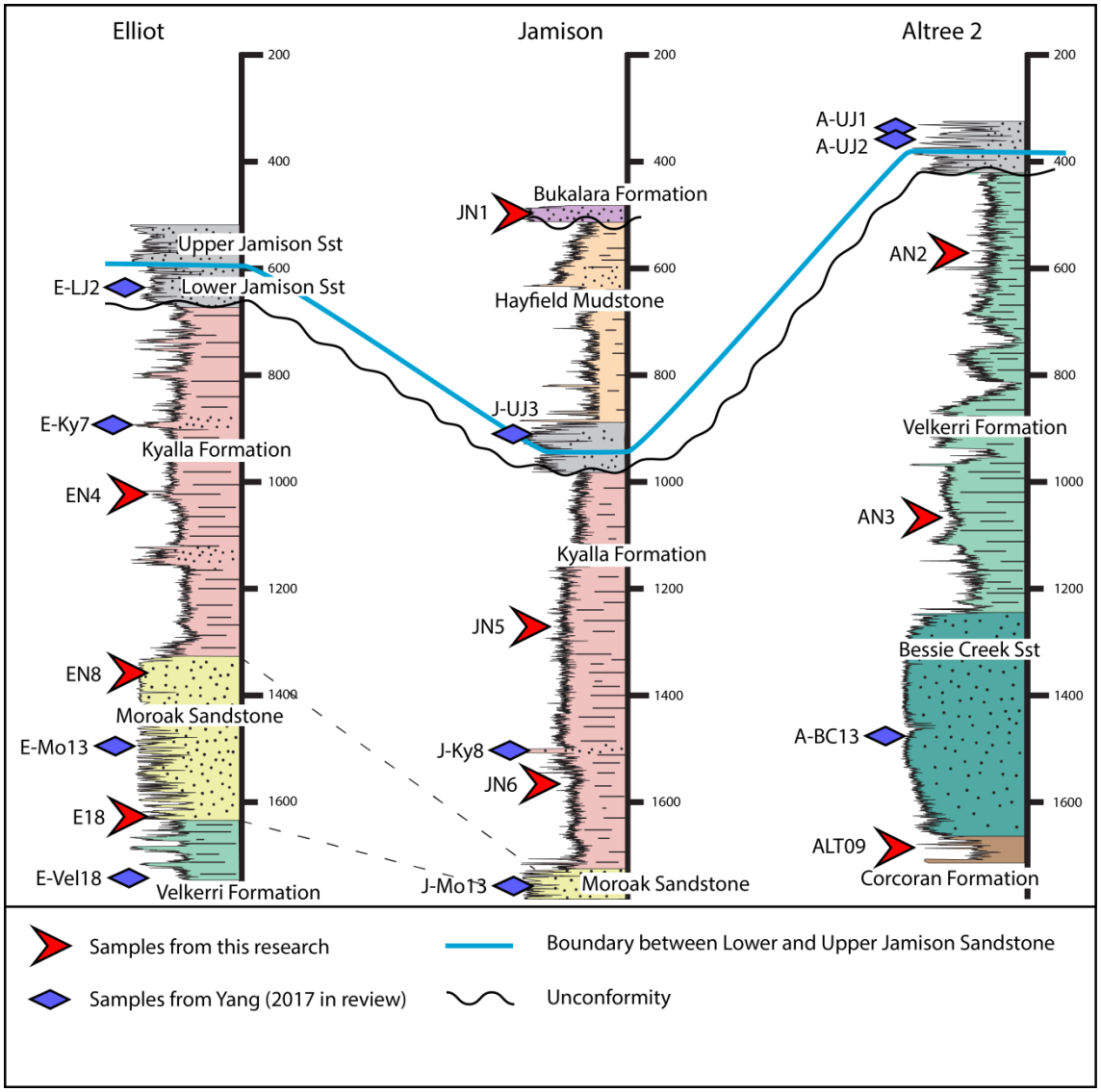

Figure 3: Stratigraphic columns interpreted from gamma-ray spectrometry of the 3 drill holes sampled in this study. Unofficially named upper and lower Jamison sandstone unit boundary follows interpretation by Gorter and Grey (2013). Red arrows indicate sandstone sample locations from this study while purple arrows indicate samples from previous studies (Yang et al., in review) used in MDS interpretations.

Zircon U-Pb analysis

Zircon U-Pb and REE data were obtained via laser ablation ICP-MS (LA-ICP-MS) on a New Wave 213 nm Nd-YAG laser coupled with the Agilent 7500cs inductively coupled plasma–mass spectrometer at Adelaide Microscopy. The laser was set to a 30 µm spot size and a frequency of 5Hz.

GEMOC GJ-1 zircons with $^{207}Pb/^{206}Pb$ age of 607.7 ± 4.3 Ma, $^{206}Pb/^{238}U$ age of 600.7 ± 1.1 Ma and $^{207}Pb/^{235}U$ age of 602.0 ± 1.0 Ma (Jackson et al., 2004) were used to correct for U-Pb instrumental fractionation. Accuracies of U-Pb data were controlled using the Plešovice zircon standard with $^{206}Pb/^{238}U$ age of 337.13 ± 0.37 Ma (Sláma et al., 2008). A total of 172 Plešovice internal standards were analysed and yielded weighted average ages of $^{206}Pb/^{238}U$ = 342.5 ± 2.5 Ma (95% confidence, MSWD = 14) and $^{206}Pb/^{207}Pb$ = 337.6 ± 6.3 Ma (95% confidence, MSWD = 0.1).

Zircon REE Analysis

In addition to the U-Pb masses used for zircon age constraints, the abundance of the following 21 elemental masses were measured: ^{31}P, ^{49}Ti, ^{89}Y, ^{90}Zr, ^{139}La, ^{140}Ce, ^{141}Pr, ^{146}Nd, ^{147}Sm, ^{153}Eu, ^{157}Gd, ^{159}Tb, ^{163}Dy, ^{165}Ho, ^{166}Er, ^{169}Tm, ^{172}Yb, ^{175}Lu, ^{178}Hf, ^{202}Hg and ^{232}Th using P as the discriminator between I and S-type granites.

Only >90% U-Pb concordant zircon grains were used in REE analysis.

Trace element concentrations were collected concurrently with U-Pb isotopic ratios.

Trace element data collected were standardised to NIST610 values as a primary standard with 91500 zircon as the secondary standard. REE data was normalised to Chondrite values taken from Taylor and McLennan (1985).

All zircon data were processed in Iolite (Paton et al., 2011) and plotted using the Excel add-in Isoplot. For U-Pb visualisation, kernel distributions and multidimensional scaling (MDS) plots were processed in R software package (Vermeesch, 2013).

Illite Slide Preparation

For the Illite Crystallinity analysis, 17 shale samples were selected over the 3 wells (Fig. 4) and were collected from the NTGS core library or obtained as fine grained material which had previously been processed by Weatherford labs.

Table 2: A list of the samples taken for Illite Crystallinity X-Ray diffraction analysis. Samples were taken at large intervals to acquire a comprehensive range of data down the entirety of the drill hole.

Well	Formation	Sample Name	Depth (m)
Altree	Up Velkerri	G1	504.0
	Mid Velkerri	DA41	665.0
	Mid Velkerri	DA43	863.0
	Low Velkerri	DA44	1110.0
	Bessie Creek	AS-1	1441.7
	Bessie Creek	ALT11	1647.3
Jamison	Hayfield	JS-1	501.9
	Hayfield	JS-3	774.8
	Up Jamison	J4	968.5
	Kyalla	JN-5	1278.4
	Kyalla	J9	1528.4
	Kyalla	J11	1695.9
Elliot	Kyalla	DE103	677.2
	Kyalla	DE104	920.5
	Kyalla	DE107	1230.6
	Moroak	ES65	1542.3
	Moroak	E18	1697.4

The samples were prepared by washing and crushing at Adelaide University as per the recommended method of Kisch, (1991). The removal of carbonates was completed by mixing the sample with a 1M sodium acetate buffered at a pH of 5 in a heat bath set at 90°C. Organics were then removed with a hypochlorite bleach solution at a pH of 9.5 in a 90°C heat bath. Solutions were then diluted, centrifuged and rinsed off a further 4 times. To isolate the <2um clay fractions, the suspended samples were centrifuged at 400rpm for 5 minutes, and pipetted on to Si slides. The slides were dried in a ventilated oven at 40°C for 48 hours and removed for XRD analysis.

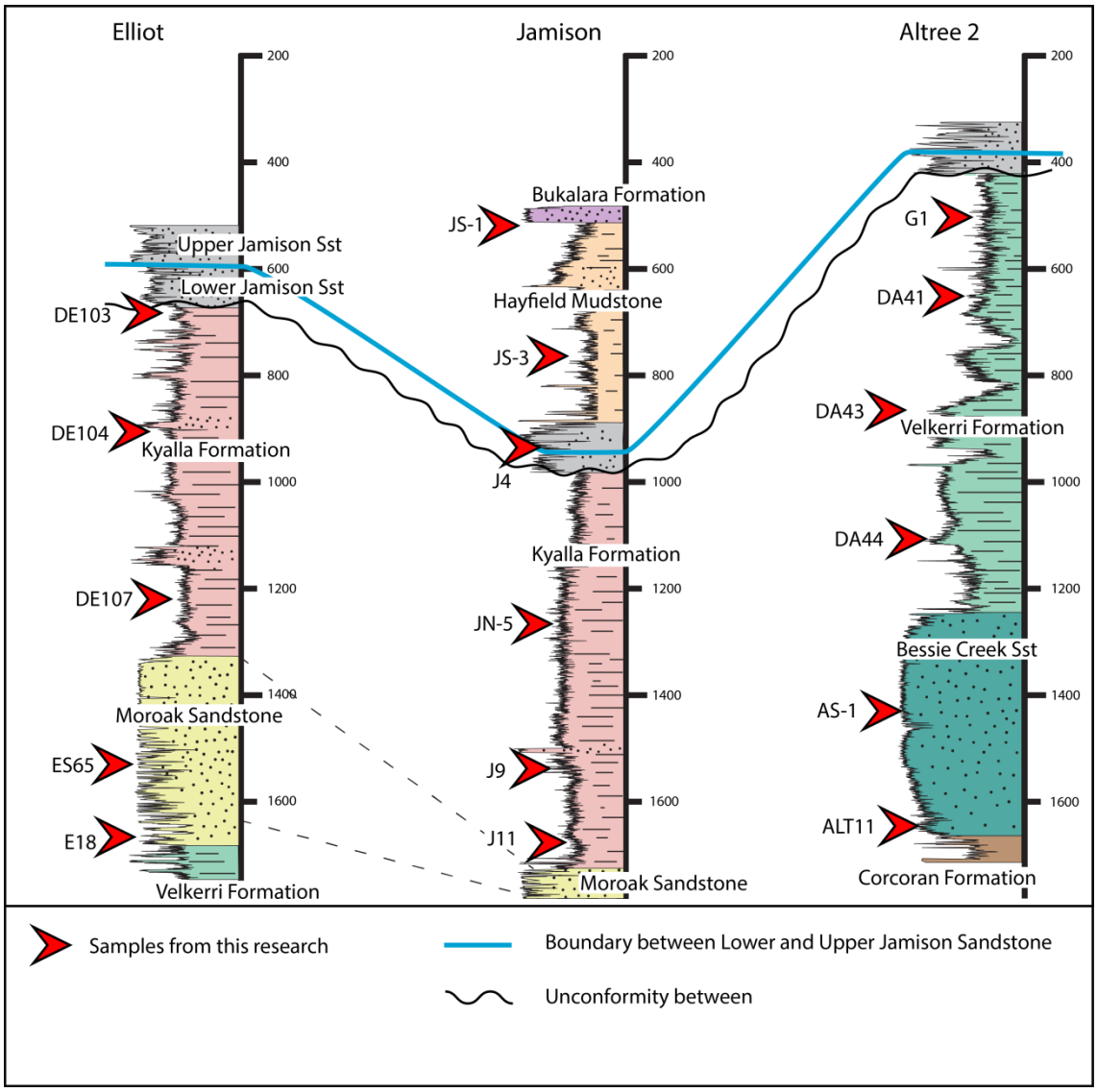

Figure 4: Stratigraphic columns interpreted from gamma-ray spectrometry of the 3 drill holes sampled in this study. Unofficially named upper and lower Jamison sandstone unit boundary follows interpretation by Gorter and Grey (2013). Red arrows indicate illite clay sample locations.

Illite Crystallinity Analysis

Analysis was completed on a Bruker D8 Advance X-Ray diffractometer at the University of Adelaide using the following settings: CuKα radiation at 40 kV and 40 mA. Slides were first run as air dried samples and again after treatment with ethylene glycol to aid in distinguishing and removing the effect of remnant smectite in the sample. For inter-laboratory calibration, values were calibrated to standardised samples

(Warr and Rice 1994) prepared by Hansberry et al. (2014) which follow the same method outlined by Warr and Rice (1994). The raw data were then converted to Crystallinity Index Standard (CIS) values and temperatures were calculated as per the equation of Kosakowski at al. (1999).

OBSERVATIONS AND RESULTS

U-Pb Geochronology

To aid in description, samples are listed in the order of formation from which they were sourced and are ordered from deepest through to shallowest formations.

Only near-concordant zircon grains were used in analyses. The concordance has been calculated by dividing the $^{206}Pb/^{238}U$ age by the $^{207}Pb/^{206}Pb$ age and multiplying by 100. Only data less than 10% discordant are shown in the U-Pb plots.

To better understand the relationships of ages, kernel distribution estimates (KDE) have been plotted (Fig. 6) which shows peak grain ages. Peak height is representative of number of grains corresponding to that age to give a visual representation of the age distributions within a sample (Vermeesch, 2014).

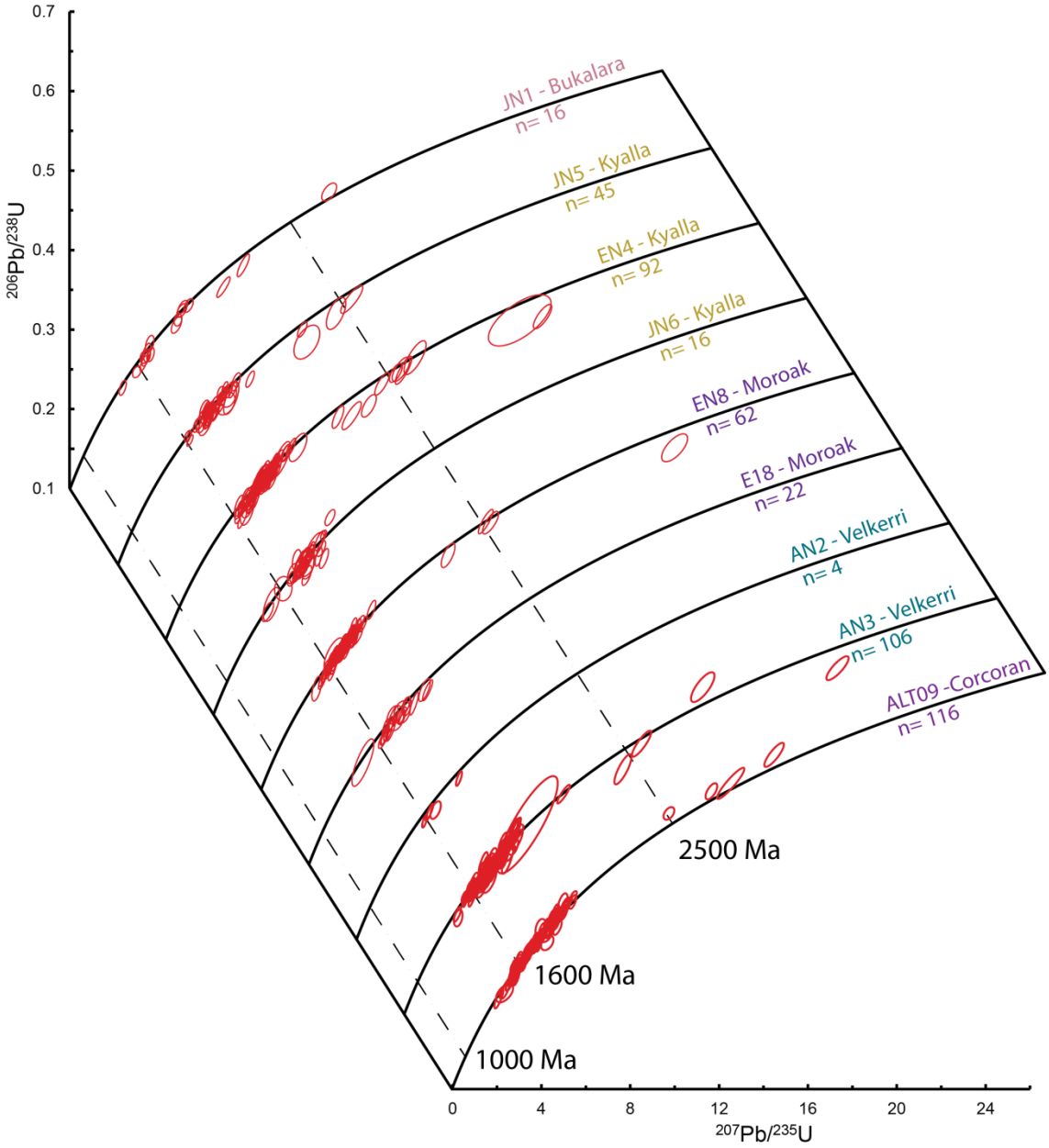

Figure 5: U-Pb Wetherill concordia plots of all samples taken from drill cores within the Beetaloo Sub-basin showing age distributions and errors.

CORCORAN FORMATION

Zircon yield was highest in the deepest sample analysed, sample ALT-09, producing the most near-concordant analyses of all samples. The grains ranged in size from 300μm to 100μm and most were elongated with some showing rounding. Oscillatory zoning patterns were present in many grains with fewer showing evidence of metamictisation. One hundred and twelve near-concordant samples yielded $^{207}Pb/^{206}Pb$ ages between 1375 Ma and 1915 Ma and produced several small kernel density peaks between these ages (Fig. 6). The youngest zircon in the sample returned a $^{207}Pb/^{206}Pb$ age of 1420 ± 37 Ma (97% concordance). Four older grains returned ages between 2702 Ma and 2342 Ma.

VELKERRI FORMATION

The zircon yield in sample AN2, a fine grained interbedded silt and sandstone, was low relative to other samples and only four >90% concordant grains were recorded. The average size for zircons in this sample is <100μm. Most grains are well rounded and do not retain their original grain shape. The youngest > 95% concordant grain returned a $^{207}Pb/^{206}Pb$ age of 1617 ± 62 Ma (95% concordant). The other three grains produced $^{207}Pb/^{206}Pb$ ages of 1598, 1652 Ma and 1853 Ma.

Zircons in the sample AN3 from the Lower Velkerri are mostly elongated and vary in size from 250um to <80um. One hundred and two analyses returned concordant $^{207}Pb/^{206}Pb$ ages between 1459 Ma and 2125Ma which produce a peak age of ca. 1770 Ma skewed towards older values. The youngest >95% concordant single grain in this sample, and the Velkerri Formation, returned a $^{207}Pb/^{206}Pb$ age of 1466 ± 25 Ma (98% concordance). A further four analyses returned Palaeo to Neo-Archean ages of 3112 Ma, 2617 Ma, 2538Ma and 2524 Ma.

MOROAK SANDSTONE

Zircons in the sample EN8 vary greatly in size from 600μm to <100μm and are rounded to sub-rounded. Internal textures and convolute structure of grains are present that may represent metamictisation. Fifty-nine grains returned $^{207}Pb/^{206}Pb$ ages between 1470 Ma and 1830 Ma with 3 samples of 2334 Ma, 2442 Ma and 2457 Ma which formed an age peak at ca. 1630 Ma and ca. 1500 Ma. A single concordant grain returned a $^{207}Pb/^{206}Pb$ age of 3049±32 Ma.

Sample E18 returned a low number of concordant grains with only 22 analyses being >90% concordant. Grains vary from 130μm to as small as 60μm along the c-axis and range from elongate-euhedral to well rounded. $^{207}Pb/^{206}Pb$ values in this sample returned ages between 1420 Ma and 1960 Ma which formed an age peak at ca. 1610 Ma skewed towards younger ages. The age of the youngest concordant grain in this formation returned a $^{207}Pb/^{206}Pb$ age of 1422 ±62 Ma (95% concordant) and comes from sample E18.

KYALLA FORMATION

The zircons in sample JN5 average around 150μm and are mostly subhedral. Analyses of these zircons revealed forty-one concordant $^{207}Pb/^{206}Pb$ ages from 2006 Ma to 1562 Ma. Another four grains returned early Palaeoproterozoic to late Neo-Archean ages from 2525 Ma to 2313 Ma. Kernel density estimate plots revealed a main peak at ca. 1800 Ma and a smaller peak at ca. 1600 Ma.

In sample EN4, zircon grains vary in shape from subhedral to well-rounded, with varying degrees of internal fracturing. Eighty-three concordant analyses returned $^{207}Pb/^{206}Pb$ ages from 1517 Ma to 2204 Ma and form the majority of grain ages with a peak at ca. 1750 Ma (shown in KDE plot Fig. 6). Seven, early Palaeoproterozoic to

Neoarchean grains, form a peak at ca. 2500 Ma with a further two samples at 2986 ± 96 Ma & 2991 ± 24 Ma.

Zircons in sample JN6, the deepest sample analysed in the Kyalla Formation, range in size from 250μm to 80μm. A contrast between well-rounded to completely euhedral, elongated grains, is present. The 35 near-concordant analyses $^{207}Pb/^{206}Pb$ ages between 1883 Ma and 1420 Ma. Kernel density estimates (Fig. 6) show a peak at ca. 1720 Ma and a small rise at ca. 1420 Ma. The age of the youngest concordant grain is 1420 ± 120 Ma ($^{206}Pb/^{238}Pb$) and comes from the sample JN5.

BUKALARA FORMATION

Zircons in the sample JN1 range from <100μm to 300μm in size and most still retain their original elongate shape with well rounded edges. The sandstone sample yielded a low number of zircons and only sixteen near-concordant analyses were produced giving $^{207}Pb/^{206}Pb$ ages between 1357 Ma and 2528 Ma. Two clusters of grains formed peaks at ca. 1850 Ma and ca. 1620 Ma (Fig. 6). The youngest near-concordant zircon from this formation yielded an age of 1357 ± 58 Ma ($^{207}Pb/^{206}Pb$).

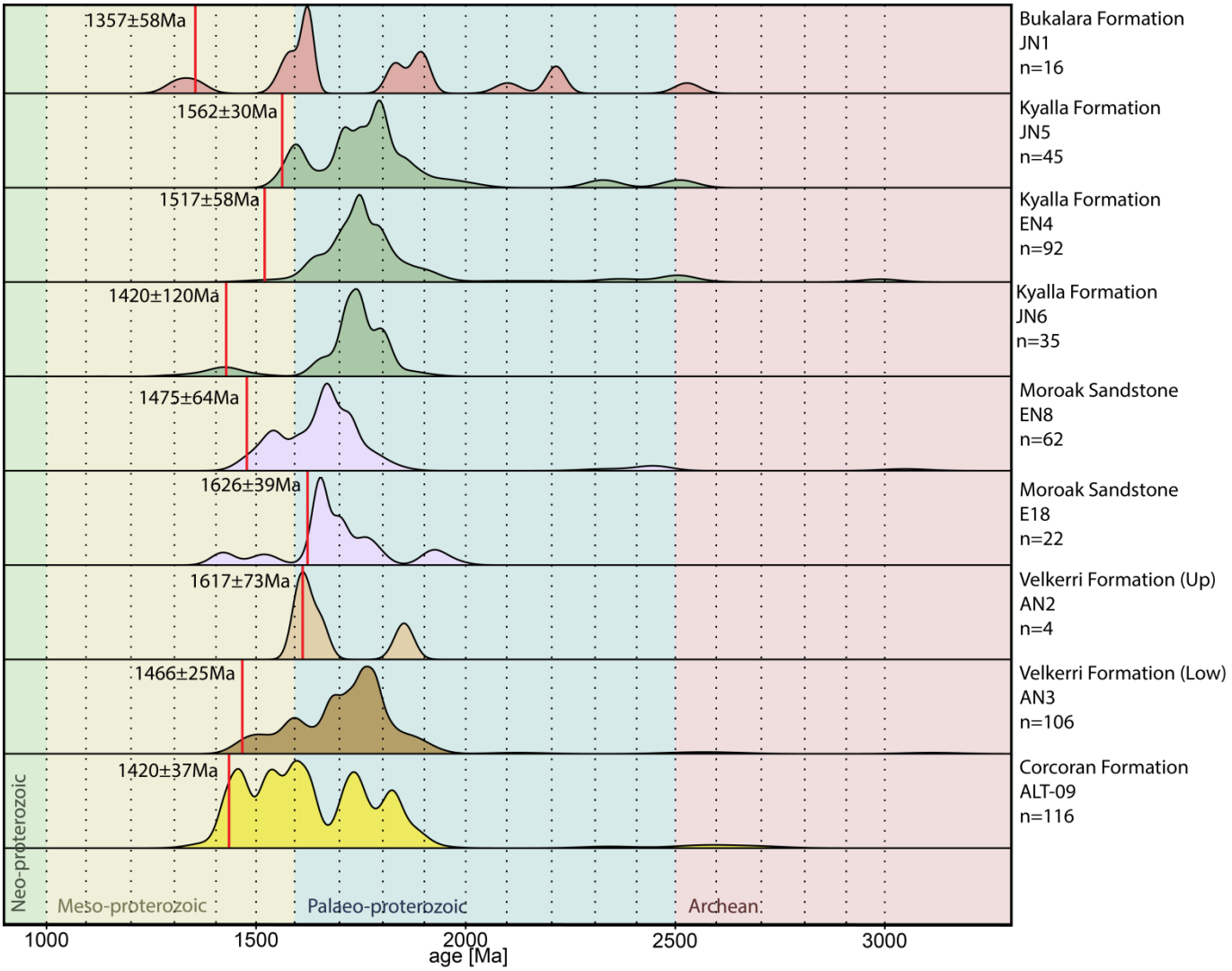

Figure 6: Kernel density estimation (KDE) plots of detrital zircon ages from samples within the Beetaloo Sub-basin drill cores. Red lines indicate youngest detrital zircon ages for each sample with error.

Zircon Trace Element

Rare earth element (REE) abundances of seventeen samples are presented in **Figure 8**.

All samples throughout all formations show a similar REE chemistry with little variance with depth.

Phosphorous concentrations in zircon

The phosphorous content in zircons is closely related to the granites in which they were formed and has been used to differentiate between I-type or S-type source rocks

(Burnham and Berry, 2017). They are distinguished by their distinct geochemical signatures due to I-type granites being predominantly igneous or infracrustal whilst S-type granites are derived from sedimentary or supracrustal sources (Chappel & White, 1992). Cumulative P concentrations of zircons are shown in **Figure 15** for each well and show the relationship with S and I-type granites found by Burnham and Berry (2017). P concentrations in zircons found in I-type granites tend to be higher and more variable than that of in S-type granite. All of the nine samples analysed show a cumulative P trend similar to that of I-type granites with a higher and more variable concentration.

The ratio of REE+Y to P concentrations in zircons has also been effectively used to discriminate between I and S-type granites. S-type granitic zircons display a strong 1:1 correlation between their molar concentrations of P and REE+Y in contrast to I-type granites which are more enriched in REE+Y. Samples have been plotted in **Figure 7** showing the relationship of these two concentrations and places them relative to known I-type and S-type granites (Burnham and Berry, 2017). Seven samples plot above the 1:1 ratio and produce values expected of I-type granites. Samples EN8 and JN6 however do plot a combination of values with a number of grains showing a propensity to follow the 1:1 ratio. Sample AN3, in the Velkerri Formation, produced two different distributions with one plotting in the I-type field showing enrichment in REE while another shows the higher P enrichment.

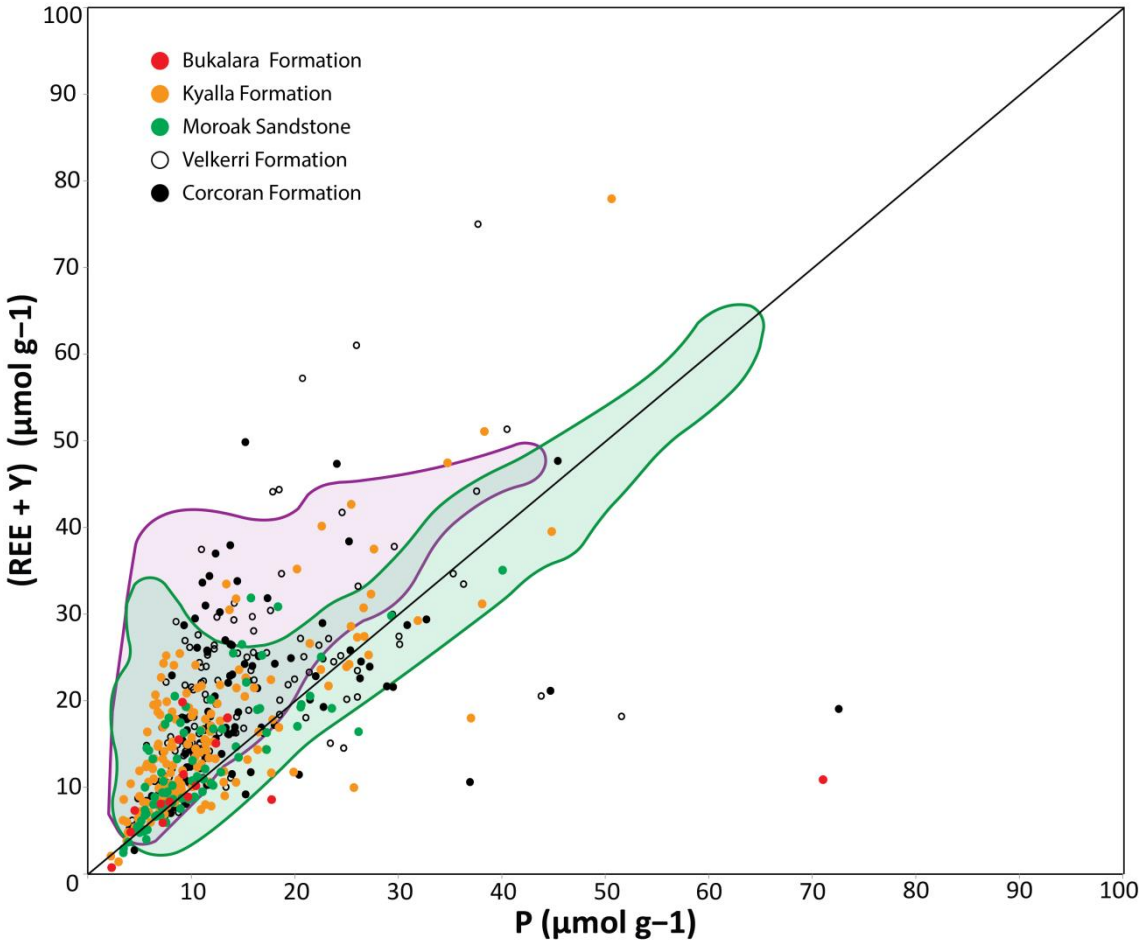

Figure 7: Plot of REE+Y vs P concentrations in zircons. S-type granitic zircons plot in the green field whilst I-type granites plot in the Purple Field (Burnham and Berry, 2017). Samples from this study are plotted in formation with no clear relationship to granite fields present.

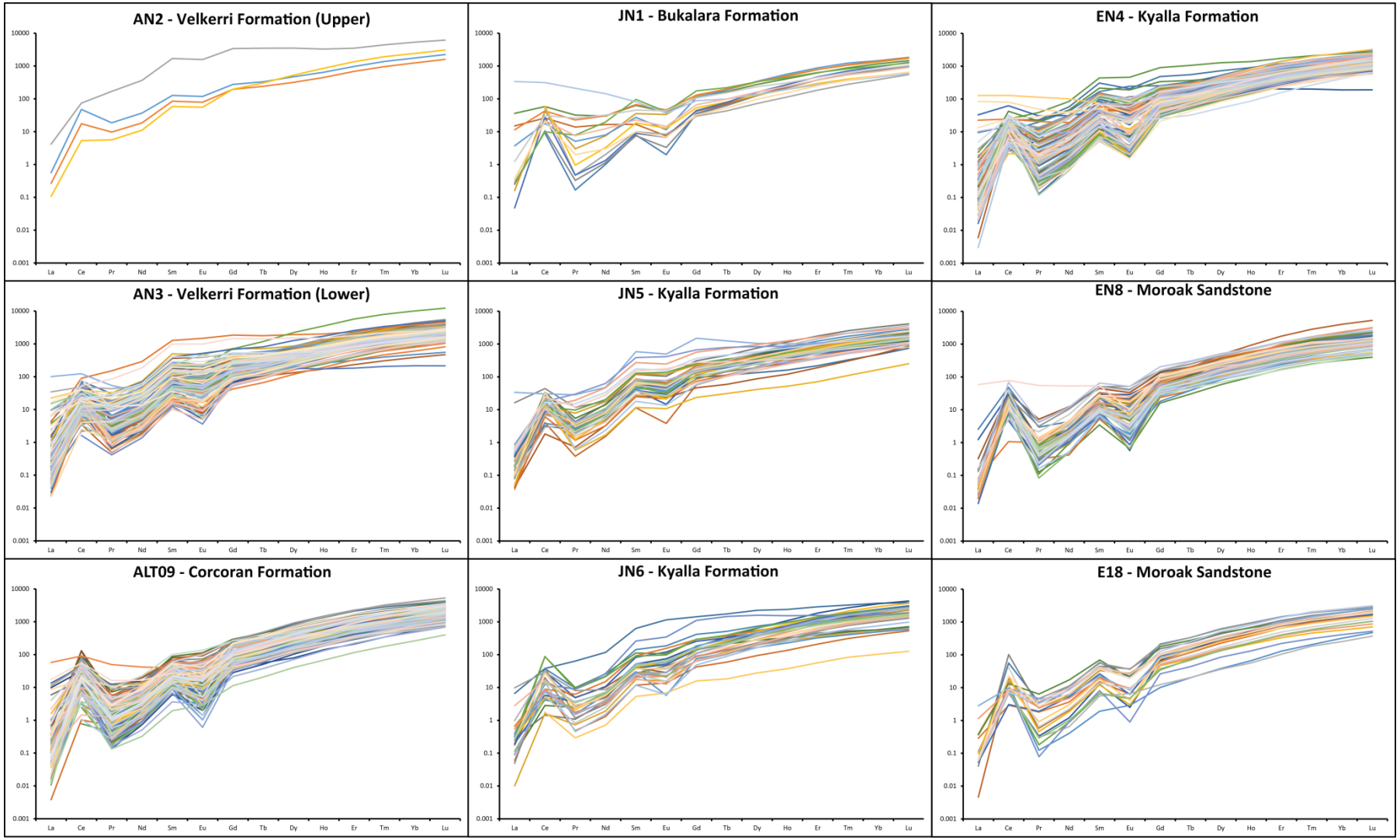

Figure 8: Chondrite normalised logarithmic REE concentrations of samples taken from Altree 2, Jamison and Elliot drill cores in the Beetaloo Sub-basin.

Table 3: List of the samples taken for Illite Crystallinity X-Ray diffraction analysis, CIS converted values and temperature calculations..

Well	Formation	Sample Name	Depth (m)	Metamorphic Zone	KI(CIS) Δ2θ	Temp (C)
Altree	Up Velk	G1	504.0	Diagenetic	0.88	48
	Mid Velk	DA41	665.0	Diagenetic	0.66	88
	Mid Velk	DA43	863.0	Diagenetic	0.46	156
	Low Velk	DA44	1110.0	Diagenetic	0.44	165
	Bessie Crk	AS-1	1441.7	Diagenetic	0.93	41
	Bessie Crk	ALT11	1647.3	Diagenetic	0.47	155
Jamison	Hayfield	JS-1	501.9	Diagenetic	0.53	129
	Hayfield	JS-3	774.8	Diagenetic	0.48	149
	Up Jamison	J4	968.5	Diagenetic	0.53	131
	Kyalla	JN-5	1278.4	Anchizone	0.38	198
	Kyalla	J9	1528.4	Diagenetic	0.74	70
	Kyalla	J11	1695.9	Diagenetic	0.46	156
Elliot	Kyalla	DE103	677.2	Diagenetic	0.63	98
	Kyalla	DE104	920.5	Diagenetic	0.70	79
	Kyalla	DE107	1230.6	Diagenetic	0.49	145
	Moroak	ES65	1542.3	Diagenetic	0.45	162
	Moroak	E18	1697.4	Anchizone	0.39	194

XRD Analysis

Crystallinity index standard (CIS) values for seventeen samples have been presented in table 3 along with their interpreted temperatures. Their spatial relationship between drill holes is shown in **Figure 2** and their present day depth relationship of each sample is shown in **Figure 4**. CIS values range between 0.39 and 0.88 which correspond with very low grade metamorphism (VLGM) within the low anchizone and deep diagenetic zones (Kübler, 1968).

When combining all three wells, a relationship between depth and temperature exists where increased depth corresponds with an increase in temperature. The Elliot well shows a fairly linear relationship. The Altree 2 and Jamison wells, although overall do tend to higher temperatures with depth, both have an excursion to higher CIS values at 1441.1m and 1528.4m respectively. In the Altree 2 well, this excursion is found in the

Bessie Creek Sandstone whereas in the Jamison well, it is found in the Kyalla formation.

DISCUSSION

Minimum depositional ages for all samples analysed in the Maiwok formation have been constrained through the cross cutting Derim Derim Dolerite. This dolerite has a SHRIMP U-Pb baddeleyite age of 1324 ± 4 Ma and cross cuts all of the formations in the Maiwok Sub-group except for the Chambers River Formation (Abbott et al., 2001). This dolerite does occur in the Beetaloo Sub-basin but dates come from samples in the Urapunga region and I have assumed that the formation correlation throughout the Roper Group is correct.

Depositional age constraints

CORCORAN FORMATION

One core sample was analysed from the Corcoran Formation and comes from the Altree 2 well. The youngest detrital zircon found in the Corcoran Formation produced a $^{206}Pb/^{238}U$ age of 1420 ± 37 Ma (97% concordance). This age is older than the 1385 ± 116 Ma found by Munson (2016) for the Bessie Creek Sandstone above. As stated, the Corcoran Formation is cross cut by the Derim-Derim Dolerite, dated as 1324 ± 4 Ma (Abbott et al., 2001), and therefore provides the minimum depositional age constraint which allows the interpretation of the Corcoran Formation depositional age between 1390 ± 27 Ma and 1324 ± 4 Ma.

VELKERRI FORMATION

Two Velkerri samples were analysed (AN2 and AN3) with both coming from the Altree 2 well. The sample AN2 yielded only four concordant zircons, only one of which >95%. The youngest single grain from both samples produced a $^{206}Pb/^{238}U$ age of 1466 ± 25 Ma (98% concordant) and comes from AN3, 556m deeper than sample AN2. This age is older than that found in the Corcoran formation and we still use the younger age found in the Corcoran Formation below and constrain the Velkerri Formation to between 1390 ± 27 Ma and 1324 ± 4 Ma.

MOROAK SANDSTONE

The two samples analysed from the Moroak Sandstone (EN8 and E18) were taken from the Elliot well and host mostly Palaeo-proterozoic zircons. The deeper sample E18 yielded a single zircon at 1626 ± 39 Ma (97% concordant) while the shallower sample EN8 an age of 1475 ± 64 Ma (99 % concordant). Once again this age is older than that found in the Corcoran formation and use the younger age found in the Corcoran Formation below and constrain the Moroak Sandstone to between 1390 ± 27 Ma and 1324 ± 4 Ma.

KYALLA FORMATION

Three samples were taken from the Kyalla formation (EN4, JN5, JN6) and come from the Elliot and Jamison wells. The samples EN4, JN5 and JN6 produced $^{206}Pb/^{238}U$ ages of 1517 ± 49 Ma (99% concordant), 1552 ± 26 Ma (98% concordant) and 1425 ± 130 Ma (98% concordant) respectively. All three of these grains produce $^{206}Pb/^{238}U$ ages older than the age constraints placed Corcoran Formation.

BUKALARA FORMATION

A single sample was taken from the Bukalara Formation and comes from the Jamison well in sample JN1. The youngest zircon analysed in this sample returned a 206Pb/238U age of 1357 ± 66 Ma (99% concordant) which is used as the maximum depositional age of this formation. The dolerite sill does not intrude this formation which has been lithostratigraphically and biostratigraphically constrained between the Ectasian and the Ediacaran based on fossil evidence and contacts with other stratigraphies (Rawlings et al., 2008).

The new data largely support the results of Yang et al. (in review) and Munson (2016), yielding comparable maximum depositional ages. The maximum depositional age of 1390 ± 27 Ma for the Corcoran Formation is a new constraint as this formation has not been previously analysed.

Figure 9: Youngest single zircon grains from this contribution used to calculate maximum depositional age plotted with weighted mean and youngest single grain ages (Yang et al., in review), dolerite U-Pb SHRIMP baddeleyite age from Abbott et al. (2001) and shale Re-Os ages from Kendall et al. (2009).

Provenance analysis through Kernel Density Estimates (KDE)

Provenance source data were obtained through previous studies listed below and are comprised of LA-ICP-MS and SHRIMP U-Pb zircon data. These potential source areas (plotted in Fig 1) are the Arnhem Province (Kositcin et al., 2015a), Pine Creek Orogen (Worden et al., 2006a, b, 2008; Carson et al., 2009; Hollis et al., 2010, 2014; Kositcin et al., 2013a; Beyer et al., 2013) and Halls Creek Orogen (Worden et al., 2008; Hollis et al., 2014) in the north, the Arunta Region (Cross et al., 2005a, b, c ; Worden et al., 2006a, b, 2008; Carson et al., 2009; Hollis et al., 2010; Bodorkos et al., 2013; Kositcin et al., 2013a, b; 2014a, b; 2015b; Beyer et al., 2013, 2015, 2016) and Mount Isa Province (Page & Sun 1998; Neumann et al, 2006, 2009; Cross et al., 2015) in the south and southeast, the Coen and Georgetown Provinces (Blewett et al., 1998; Hoskin & Black 2000; Kositcin et al., 2009) in the far east and the Musgrave Province (Wade, 2006) in the far south. The Mount Isa provinces the Eastern Fold Belt (EFB) and the Western and Kathleen Fold Belts (WFB&KFB) have been treated as two individual units in this study as they have different tectonic histories and do not share the same zircon age distributions (Page and Sun, 1998; Betts and Giles, 2006; Neumann et al, 2006, 2009; Duncan et al, 2006; Bierlein et al, 2011).

CORCORAN FORMATION

In **Figure 10** the Corcoran formations 116 zircons, from sample ALT09, show a wide range of peak ages. Five distinct peaks at ca 1825 Ma, ca 1730 Ma, ca 1605 Ma, ca 1550 Ma and ca 1460 Ma exist. No age spectra of surrounding provenances match that of the Corcoran Formation leading to the interpretation of multiple sediment sources. The two oldest peaks return ages similar to that of the Gawler Province and the

Kathleen and Western Orogens while the peak at ca. 1605 Ma is close to the peak age found in the Coen and Georgetown Orogens. The lack of Mesoproterozoic and Archean ages found in the Gawler Province tends to favour the eastern provinces as source regions.

VELKERRI FORMATION

Kernel density curves for the Velkerri Formation sample from the Altree 2 drill core (AN3) produce a main age peak at ca. 1765 Ma and secondary and tertiary peaks at ca. 1685 Ma and ca. 1600 Ma. The Corcoran and Velkerri Formations, separated by the Bessie Creek sandstone, show little resemblance in their peak distribution indicating a change in sediment source. The main peak age of the Velkerri matches the Arunta Provence KDE curve with both showing similar secondary peaks at ca. 1630 Ma indicating a possible sediment source.

MOROAK SANDSTONE

The two Moroak sandstone samples (EN8 and E18), both from the Elliot well, produce a main age peak between ca. 1660 Ma and ca. 1670 Ma. The main peak ages closely resemble one another although the samples show distinctly different ages either side of the peak. The lower (E18) sample has a peak at ca 1410 Ma and at ca 1920 Ma while the sample (EN8) above has small peaks at ca. 1730 Ma and ca. 1550 Ma. The difference in peak ages is likely due to the small sampling size in the sample E18. A single 1422 Ma sample has produced a visible peak showing the effect of a small sample size.

KYALLA FORMATION

The Kyalla formation consists of three samples, highlighted green in the KDE plot. The two lower samples, JN6 and EN4, show similar trends with a main peak at ca 1730 Ma, a secondary peak at ca 1800 Ma and a smaller peak at ca 1650 Ma. The lower JN6 has a spread of ages to the Mesoproterozoic whilst sample EN4 shows a number of grains with ages from the early Palaeoproterozoic to Archean.

The shallower JN5 sample produces a marginally different peak distribution with its main peak at ca 1800 Ma, a secondary peak at ca 1710 Ma and a third, smaller peak at 1600 Ma. Although the peak ages are different, the distribution of values is similar to that of the EN4 sample below. The Kyalla sample does not show a large variance with depth and this change may be explained by the small number of analyses per sample.

When comparing with the formation below, the main peak shifts from ca 1660 Ma in the Moroak to the ca 1750 Ma peak of the Kyalla demonstrating a source change.

The peak at ca 1750 Ma and smaller peak at ca 1650 Ma both coincide with the peaks present in the Mount Isa Province, most notably the Kathleen and Western Orogenies.

BUKALARA FORMATION

The sample obtained from the Bukalara Formation has an age distribution which covers a wide range from Mesoproterozoic to late Archean. Yang et al. (in review) and Munson (2016) observed a lack of older Palaeoproterozoic and Archean zircons in the ungrouped sediments contrasting the ages found in the Bukalara Formation. This indicates a possible shift in provenance to a source more similar to those found in the Maiwok subgroup although due to the sample only producing 16 concordant analyses, this is difficult to be certain until more data are obtained from the Bukalara Formation.

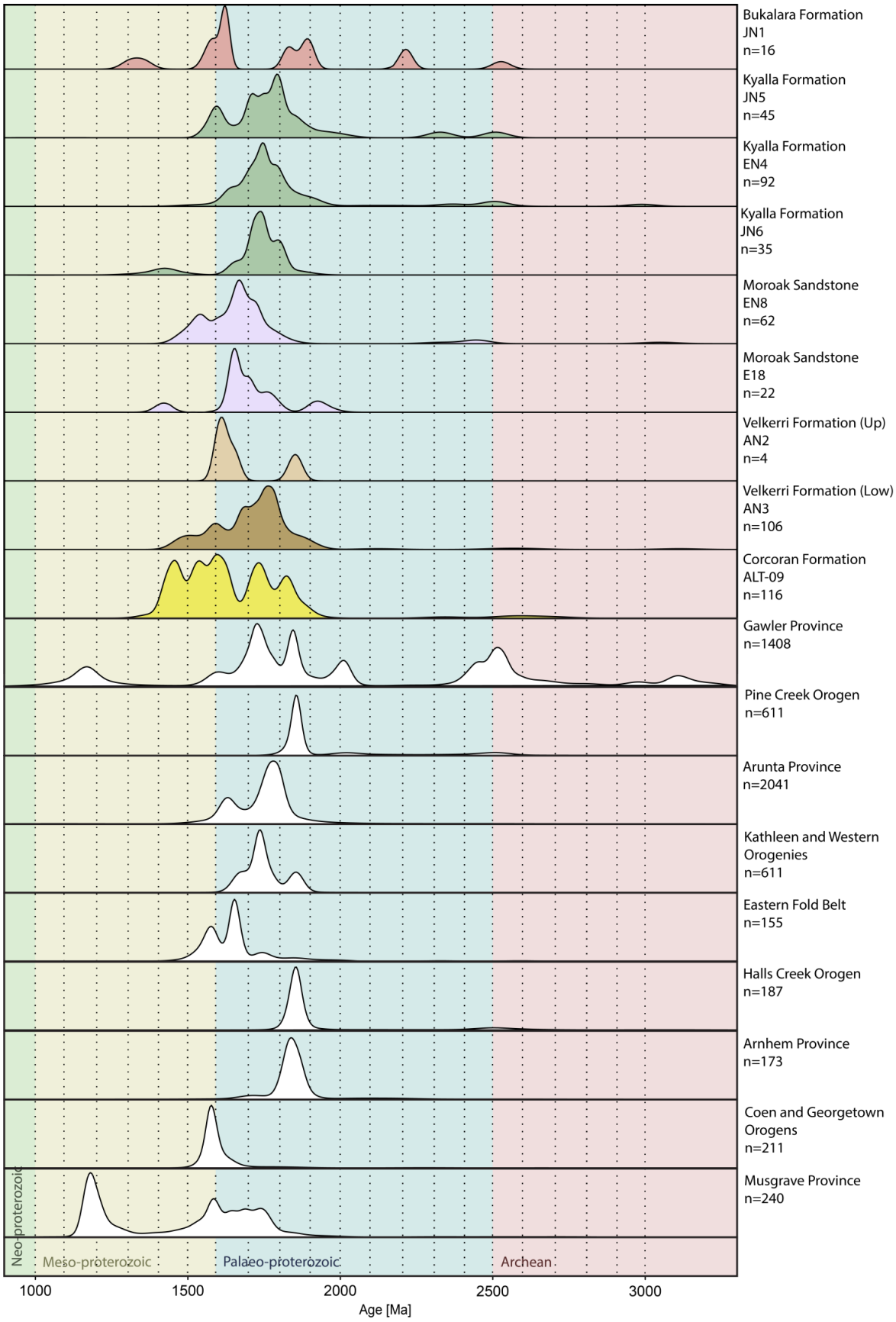

Figure 10: Kernel density estimation (KDE) plots of detrital zircon ages from Beetaloo Sub-basin samples in this study compared with potential source areas.

Multi-Dimensional Scaling (MDS)

A Multi-Dimensional Scaling (MDS) plot is used to show how similar or dissimilar a set of samples are in a data set. The technique was first proposed by Vermeesch (2013) where it was used for detrital zircon analysis. The technique uses the Kolmogorov-Smirnov (K-S) test to quantify the dissimilarity (D-value) between two age distributions. This value can then be used to form a matrix of n dimensions ('n' being the number of samples) and plotted as a two dimensional, MDS plot. In the MDS plot, the closer two values are, the least dissimilar their distributions are. When many samples are plotted the two samples with the least dissimilar distributions are connected by a solid line and the next two least dissimilar samples are connected by a dashed line. Another tool used in provenance analysis is the addition of age data in an MDS plot. To aid in visualising age distributions I have followed the method by Spencer and Kirkland (2016) which involved plotting KDE age peaks for all the Beetaloo Basin samples on an MDS plot (Fig. 12 & Fig. 13). This method has been used on this suite of samples previously by Yang et al. (in review).

Figure 11 shows the MDS plot of all the data from this research. Eight samples are plotted with the two Velkerri Formation samples (AN2 and AN3) being combined due to sample AN2 having a low number of analyses. Two groupings of samples are recognized which shows the Moroak and Corcoran Formations grouping together whilst the three samples from the Kyalla Formation showing a close relationship. The Velkerri Formation plots between these two groups and the Bukalara Formation does not plot proximal to any samples showing no close relationships.

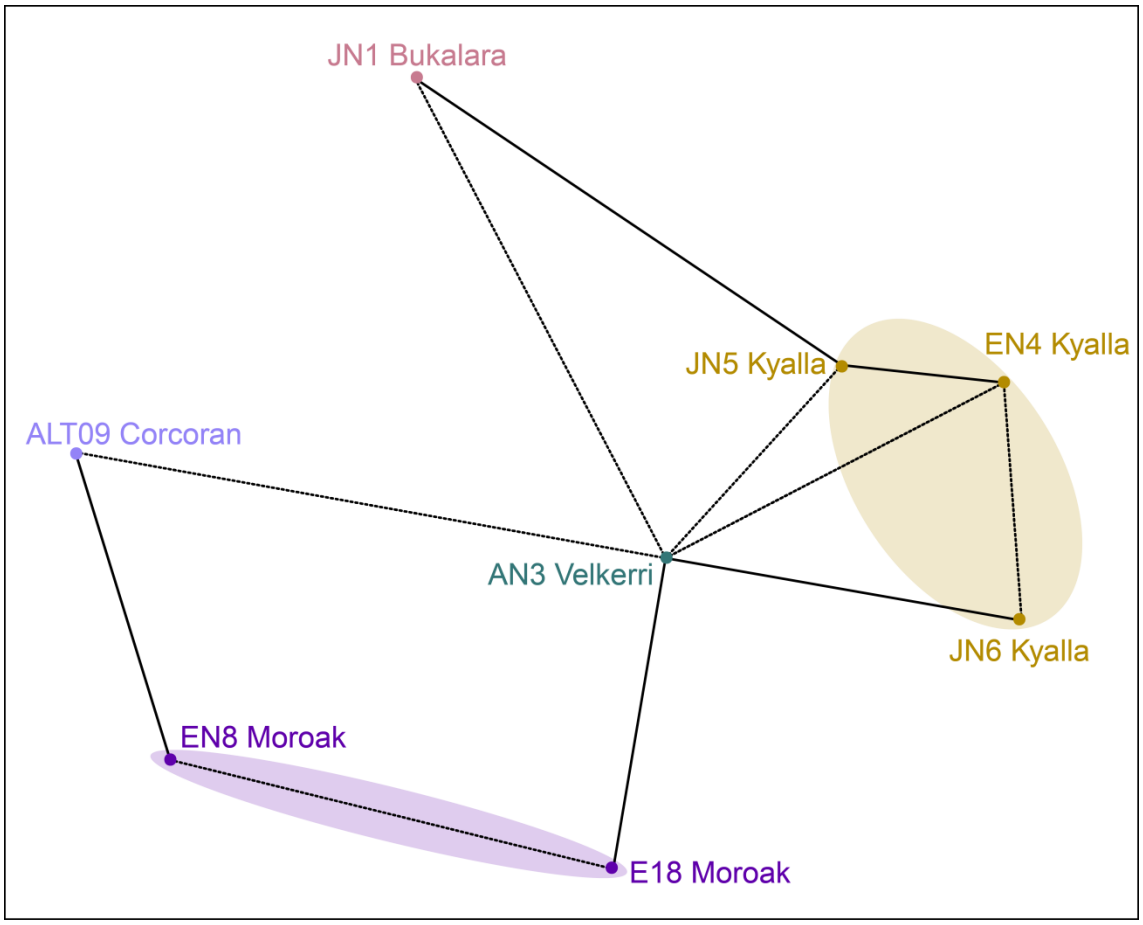

Figure 11: MDS plot of 8 samples analysed in this study with sample AN2 from the Velkerri not represented due to small sample size (4 analyses). Samples in closer proximity are less dissimilar in zircon age distributions. Kyalla formation samples have been highlighted yellow whilst Moroak sandstone samples have been highlighted purple.

Figure 12 (below) has been used to compare the relationship of the nine samples found in this study, the seventeen samples found previously by Yang et al. (in review), the six by Munson (2016) and a single sample by Fanning (2012). The Maiwok Subgroup samples from this study all plot between the ca. 1589 Ma and 1728 Ma ages showing a spread in sediment ages. A trend is apparent which shows the deeper Corcoran and Bessie Creek formations plotting closer to the ca. 1589 Ma marker and the shallower formations above plotting nearer to the ca. 1728 Ma marker. This shows a development of increasing source age with time. The exception however is the Elliot sample (EN8) from the Moroak Sandstone which plots closer to the ca 1589 Ma marker. This is to be expected from the peak of young ca. 1550 Ma ages visible in the KDE plot.

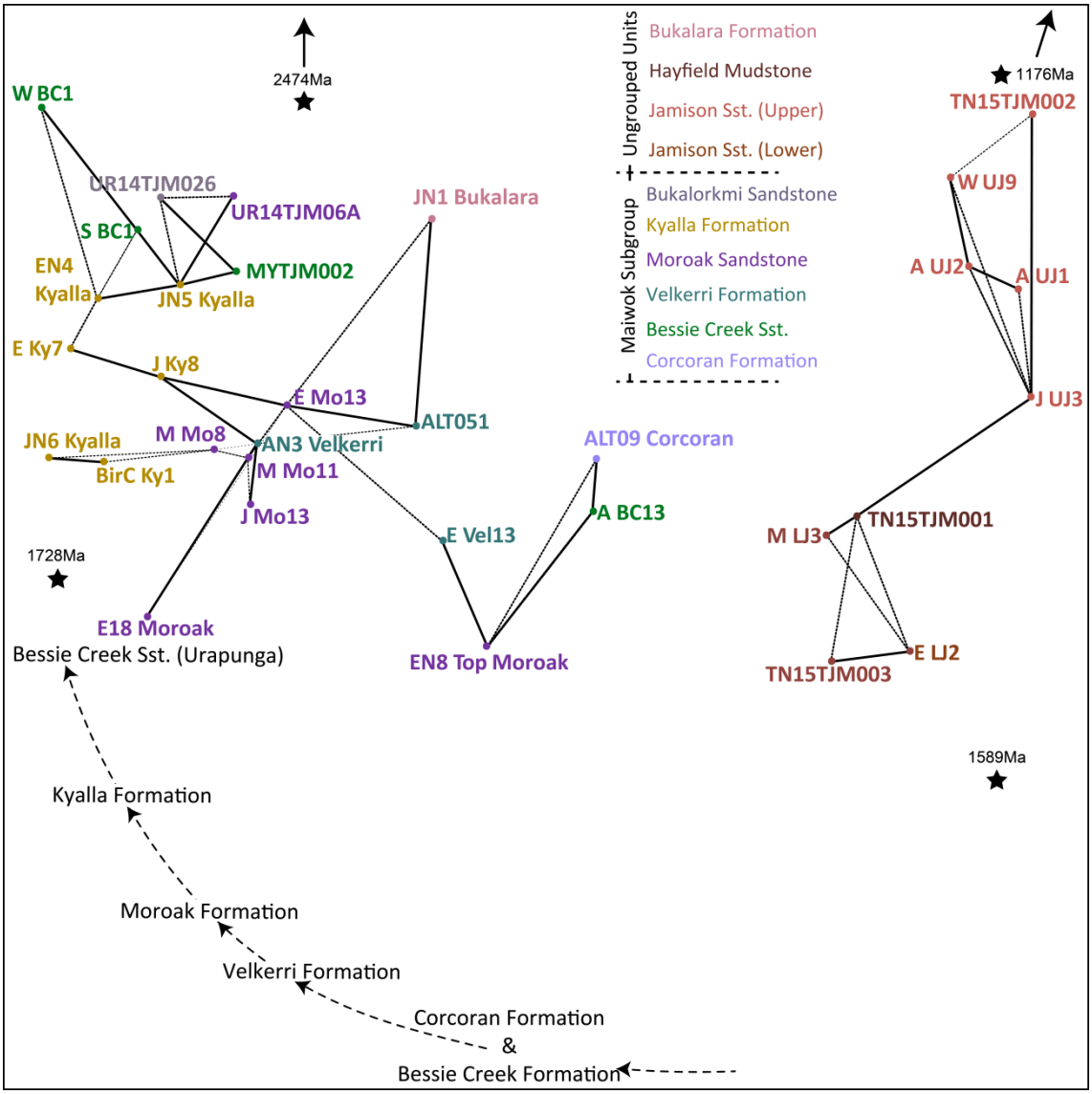

Figure 12: MDS plot of samples from Beetaloo Sub-basin this study compared with Beetaloo Sub-basin samples found in previous studies (Yang et al., in review; Munson, 2016; Fanning, 2012) and Urapunga region (Munson, 2016). Samples in this study listed with formation name. Samples plotting closest are least dissimilar and are connected by a solid black line, the next two least dissimilar are connected by a dashed line. The samples in the Beetaloo Sub-basin show a progression from younger ages (right of plot) to older ages (left of plot) when moving up formation. Stars indicate zircon age peaks found by KD estimates of all Beetaloo Sub-basin analyses.

The deeper sequences of the Maiwok Subgroup show a close relationship exists between the Corcoran Formation sample (ALT09) from this study and the Bessie Creek Formation sample (A BC13) which lies conformably above. Due to their close proximity I interpret that these two formations have a similar sediment source. This relationship also adds weight to the suggestion that the Walton High acts as a provenance boundary between the Beetaloo Basin and the Urapunga Region to the north (Yang et al., in review). In the Velkerri Formation, sample (AN3) plots adjacent to the older Moroak Sandstone samples but still close to the Velkerri Formation samples found by Yang et al. (in review) and Fanning (2012) which may indicate a transition or mixture of sources.

Figure 13 (below) shows the relationship between all of the Beetaloo Basin samples including those from Yang et al. (in review), Munson (2016) and Fanning (2012), grouped in their formations, and the suggested source provenances. All of the formations within the Maiwok Sub-group plot between the Southern and Eastern provinces and indicate a change in source throughout the Maiwok Subgroup from Eastern Fold Belt sources, through the Arunta and to Kathleen and Western Fold Belt sources with time. This relationship of increasing detrital zircon age with moving up sequence has been observed by Yang et al. (in review) and is confirmed with the addition of this new suite of data.

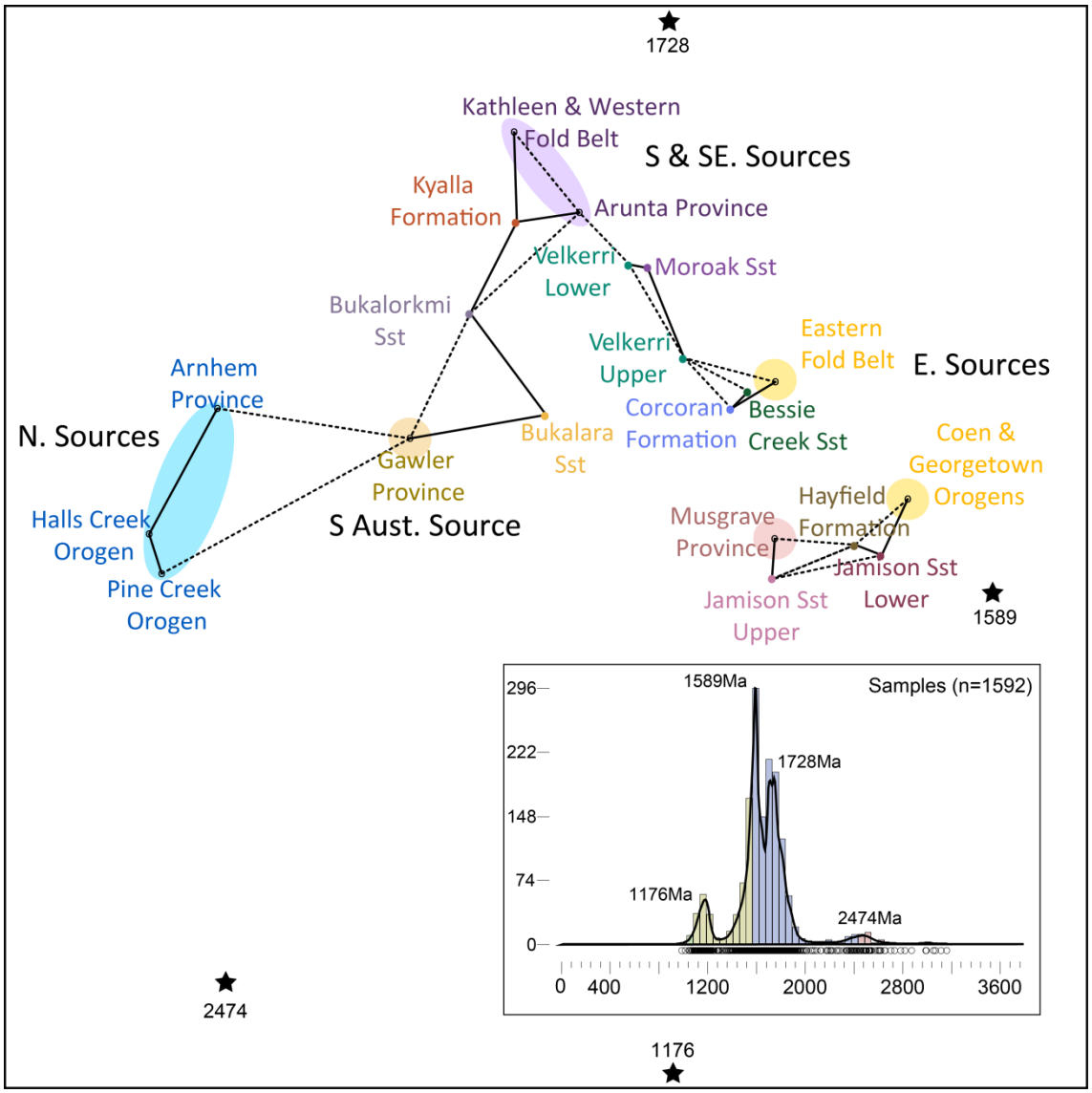

Figure 13: MDS plot of all samples from this study and previous studies (Yang et al., in review; Munson, 2016) from the Beetaloo Sub-basin grouped into their formation compared to suggested province data. Formations in the Maiwok Sub-group show a progression from the Eastern Fold belt towards the Kathleen and Western Fold Belt moving up in sequence from Corcoran to Kyalla formations.

Rare earth elemental concentrations

To constrain REE values, F**igure 14** shows the REE values for samples combined into formation. These concentrations were sub-divided into ages which are representative of the main peak ages found for all grains using kernel density estimates.

The samples do not display marked variance with age or formation showing homogeneity throughout the samples. All samples show enrichment in Ce with low La and Pr values as expected of zircon REE signatures.

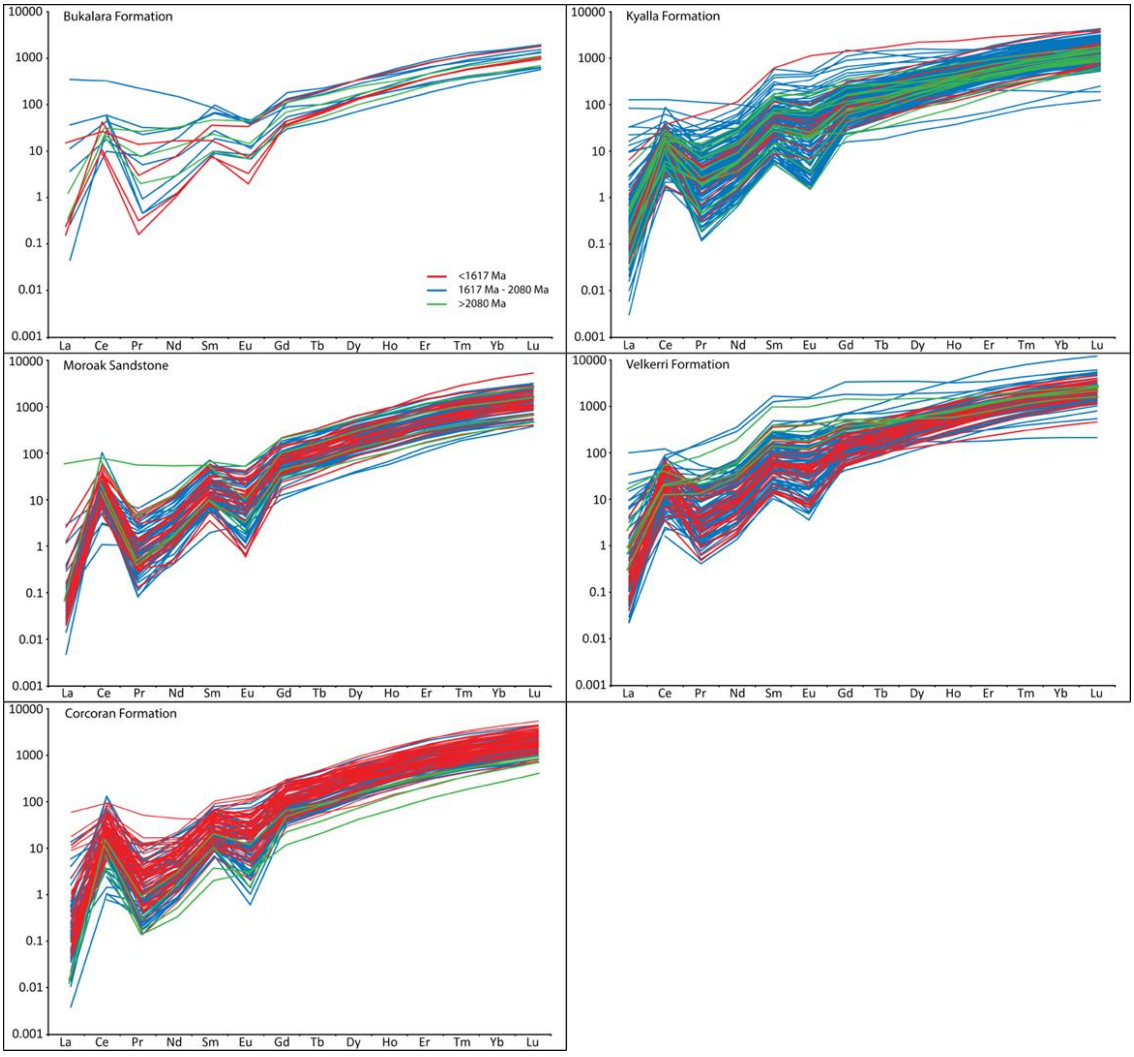

Figure 14: REE concentration plot. Samples normalised to chondrite values and plotted in formation. Age peaks determined by KDE plot of all samples used to create age brackets.

Phosphorous concentrations for granite discrimination

The cumulative P concentrations within the Maiwok Sub-group formations produce a plot which appears to exclude S-type granites as the source for the Beetaloo Basin. Zircons found throughout the basin do suggest that multiple source regions contributed to basin infill, due to the broad spectrum of ages, although no clear change in P variance exists within the different age distributions (Fig. 15). This plot excludes all age peaks from S-type granitic sources indicating that the zircons found within the basin are derived from I-type granites of all ages.

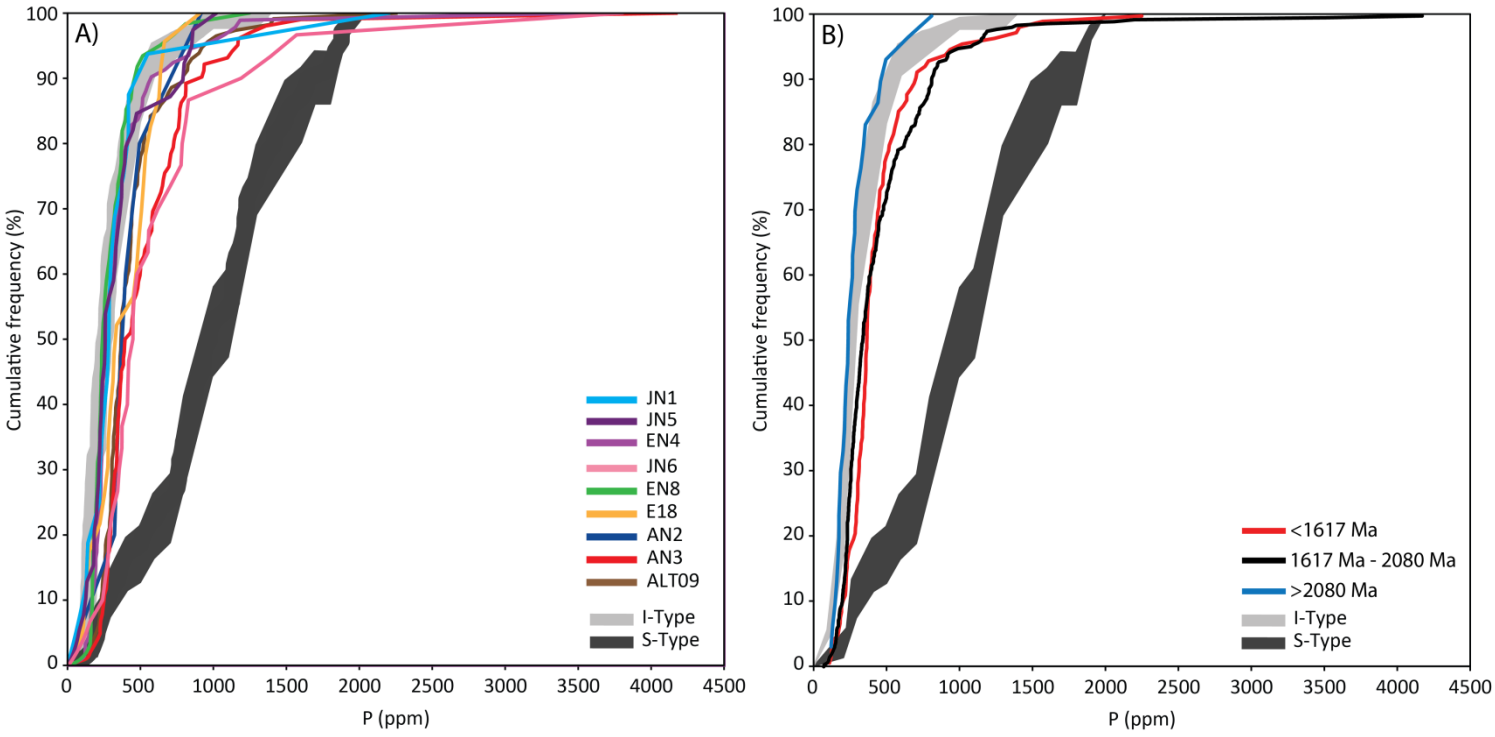

Figure 15: A) Cumulative P plot of all formations compared to I-type and S-type granite cumulative P signatures (Burnham and Berry 2017) with samples showing a mostly I-type granite signature in all samples. B) Cumulative P plot with samples grouped by zircon age peaks of all Beetaloo Sub-basin samples. When discriminating by age, samples produce strong I-type granite signatures.

When observing the relationship between the concentrations of REE + Y and P in zircons separated by age (Fig. 16), grains <1617 Ma plot mostly in the I-type granite field with a small portion of grains below or following the 1:1 line confirming the I-type source for this age group of zircons. Zircons between 1617 Ma and 2080 Ma show a variety of values and the majority plot in the mutually inclusive field of I-type and S-type granites showing a possible mixing of sources. The mainly I-type granitic sources suggested by the cumulative P and REE + Y vs P plots indicate arc-related magmatic sources from the Neo-Archean to the Meso-Proterozoic. This arc-type magmatism is recognised in the chemical signatures of the Arunta Province, Gawler Graton (Giles et al., 2002), Georgetown Orogen and Mount Isa Regions (Blewett and Black, 1998) which does not rule them out as provenance sources.

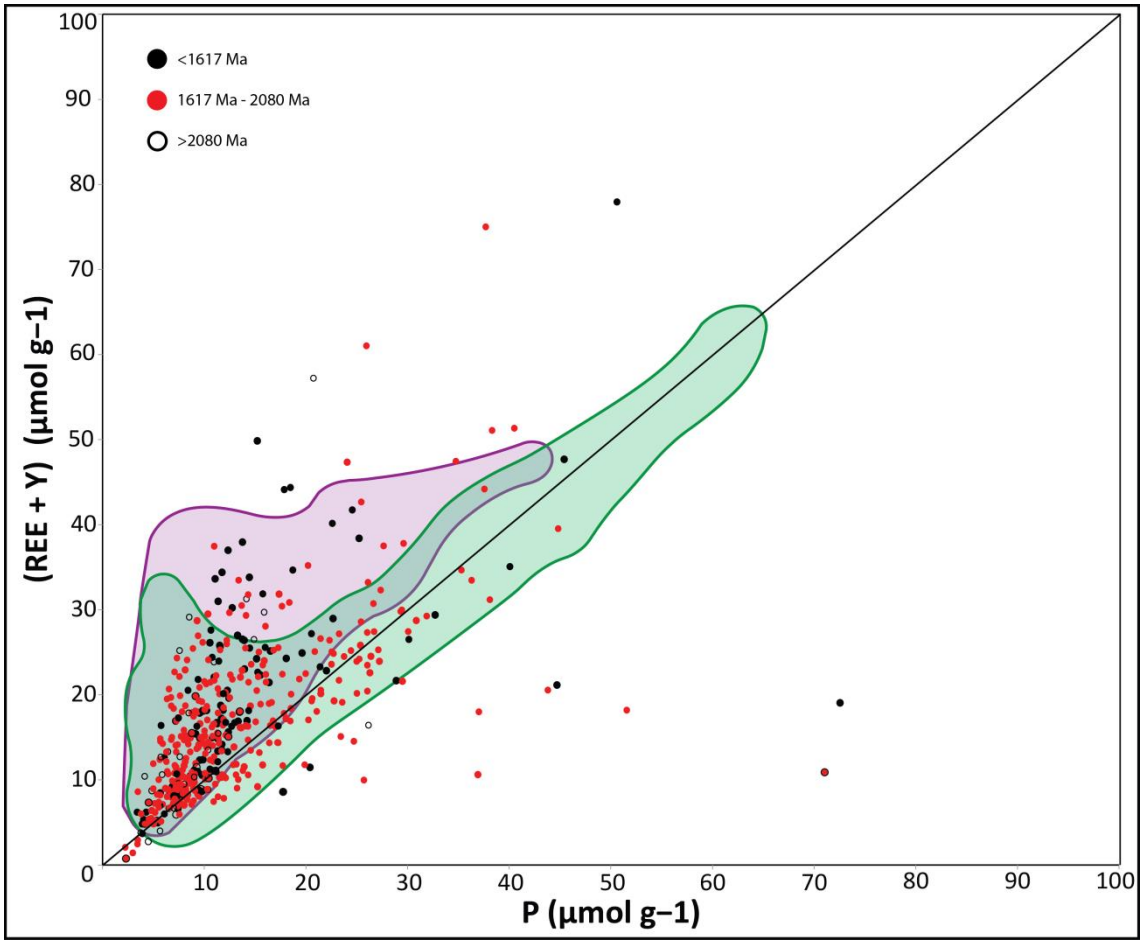

Figure 16: REE+Y vs P plot of all Beetaloo Sub-basin samples collected in this study grouped into main age peaks. Green shape indicates S-type granite field, purple indicates I-type granite field. No strong relationship exists between age groups and granite types. 1617 Ma to 2080 Ma granites do produce several analyses which follow the 1:1 correlation line indicative of an enrichment in P.

XRD downhole temperature analysis

The illite crystallinity method uses X-Ray Diffraction (XRD) to constrain the temperature conditions of very low grade metamorphism (Frey, 1987; Frey et al., 1980; Mählmann et al., 2012). The effect of deep burial and initial metamorphism of clays causes an alteration from expandable smectite to non-expandable illite (Kennedy et al., 2014). Illitization is the measurable process in smectite where by Al is substituted for Si in its tetrahedral sheets, smectite becomes dehydrated, its expandable interlayer collapses and exchangeable ions are replaced by fixed K+ and/or NH4+ (Clauer et al., 2014; Kennedy et al., 2014; Lindgreen et al., 2000). Previous studies have shown relationships between increasing temperature and illitization although there are many factors which can contribute to the altering values such as tectonic stresses, rate of heating, fluid pressure, lithology, and original clay chemistry (Frey, 1987; Underwood et al., 1993; Kübler and Jaboyedoff, 2000; Clauer et al., 2014). Illite crystallinity is measured through XRD as the 'full width at half-peak height' of the 10-Å illite peak and is expressed in units of $\Delta°2\theta$ (Kisch and Frey, 1987; Kübler, 1968; Warr et al., 1996). This value is then calibrated to a set of rock standards and converted to the 'Kübler-Index' (Kübler, 1968). Warr and Rice (1994) proposed a technique to assist in inter-laboratory calibration of data. This is done through sample calibration to a set of rock chip standards which is then presented as the 'Crystallinity Index Standard'. This is the method I have chosen and therefore have presented my data as CIS values. Temperature values have been calculated per the equation of Kosakowski at al. (1999). All three wells show an overall decrease in CIS values with depth which correlates with an increase in temperature. The Altree 2 and Jamison well both show a large shift towards higher CIS values at 1441m and 1528m deep respectively. The cold shift is

colder than present day temperatures and is likely due to errors in sample preparation. The Altree 2 well shows a temperature change from 48°C at the top of the well (504m) to a calculated 155°C at 1647m although a higher 165°C is measured at 1110m, these temperatures correlate with low anchizone to deep diagenetic metamorphic facies. The bottom-hole temperature in this well was measured to be 84°C at the time of drilling. Samples in the Jamison well also returned values in the low anchizone to deep diagenetic metamorphic facies with temperatures ranging from 129°C at 501m to 198°C at 1278m. The deepest sample (J11 at 1695.9m) returned a CIS value of 0.24 which correlates to a temperature of 156°C and is 42°C colder than the sample 417m above, this shift to lower CIS values is likely due to variance in mineralogy. The Jamison well has a present day bottom-hole temperature of 90°C at a depth of 1769m. The Elliot well returned the most linear values of all three wells and also the hottest temperature at the bottom of the well. Temperatures ranging from 98°C at 677m to 194°C at 1697m show an increase of 94°C over 1020m of depth. The Elliot well has a present day bottom-hole temperature of 84°C at a depth of 1729m. Amount of cover removed from present day drill holes was calculated by dividing the difference between present day bottom-hole temperatures and the maximum XRD recorded bottom-hole temperatures by the present day geothermal gradient. Assuming a surface temperature of 25°C I have calculated that the Altree 2 well has had 2050m of cover removed using a present day geothermal gradient of 34.7°C/ km. The Jamison well returned a value of 1790m of cover removed using a present day geothermal gradient of 36.7°C/km. The Elliot well returned the highest value with 2680m of cover removed relative to present day indicating that the southern region of the Beetaloo Sub-basin has experienced greater uplift.

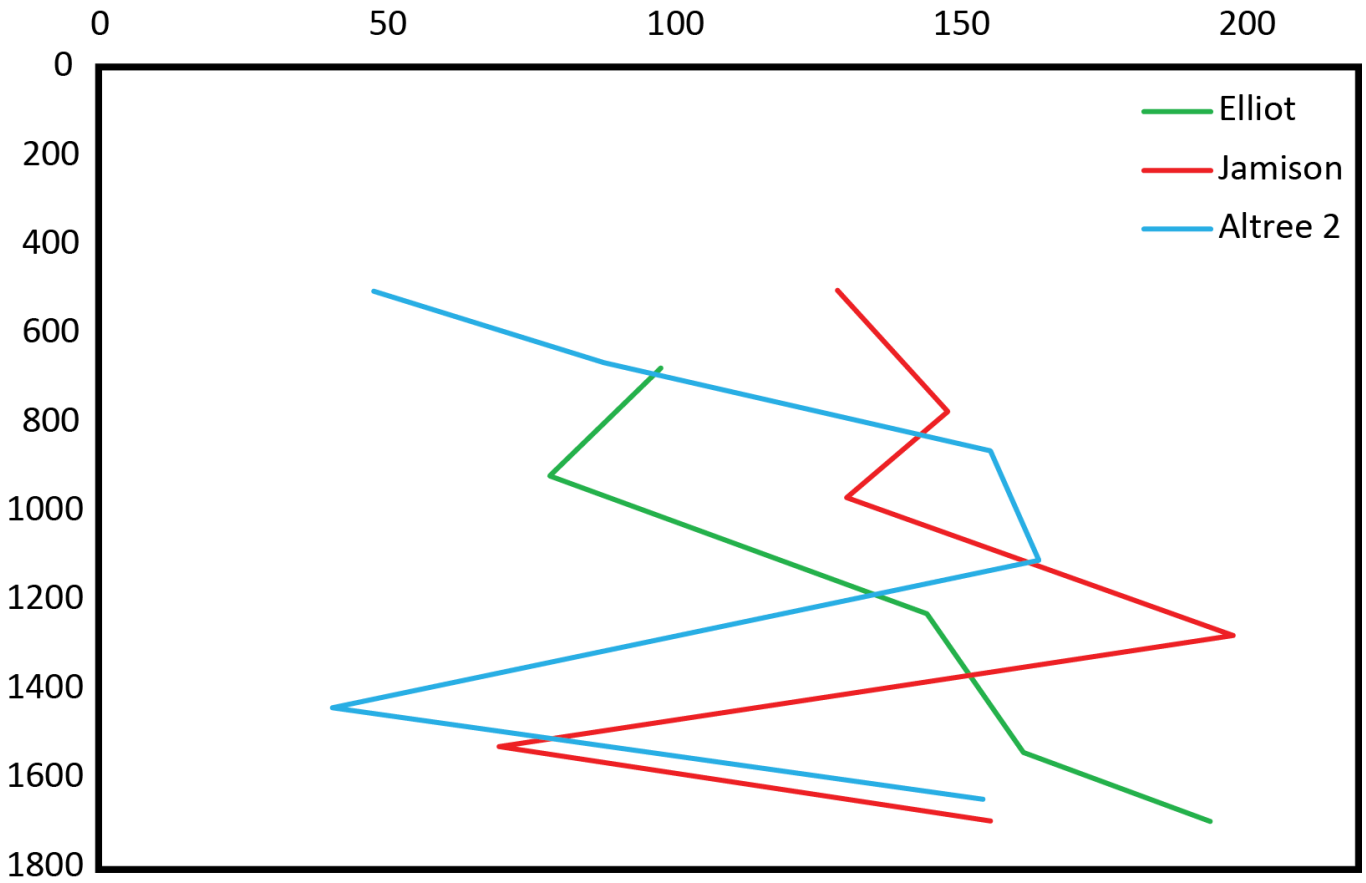

Figure 17: Temperature vs depth plot calculated through XRD analysis on illite. Both Altree 2 and Jamison show a cold excursion at 1441m and 1528m respectively. Altree 2 and Elliot wells show an increase of temperature with depth greater than present day values whilst the Jamison well shows a lower than present day geothermal gradient.

CONCLUSIONS

- New constraints have been placed on the age of deposition of the Corcoran formation to between 1390 ± 27 Ma and 1324 ± 4 Ma whilst other data supports the results of Yang et al. (in review) and Munson (2016), yielding comparable maximum depositional ages.
- Within the Beetaloo Sub-basin the probable source for Corcoran formation is the Eastern Fold Belt of the Mount Isa Province. The Velkerri Formation above contains mostly ca. 1765 Ma Zircons and displays a likeness to the Arunta Province and Eastern Fold Belt. The Moroak Sandstone was sourced from primarily Arunta Provincial sediments with some derived from the Eastern Fold Belt. The Kyalla formation shows a likely sediment source from the Arunta and the Kathleen and Western Fold Belts of Mount Isa. This changing of source regions indicates a shortening of sediment pathways with time.
- Although REE signatures provided little insight, P concentrations enabled the discrimination of zircons to mostly I-type granitic sources. This shows a relationship to arc-type magmatic granites throughout the Maiwok Sub-group.
- The Beetaloo Basin has experienced differing amounts of cover removal with spatial variations. Through illite crystallinity analysis, I have determined that the southern extent of the Beetaloo sub-basin has experienced more uplift than in the north which is currently the deepest part of the basin. Due to the large variance in illite crystallinity values down-hole a higher resolution study is recommended.

ACKNOWLEDGMENTS

I am grateful for the funding from Santos and Centre for Tectonics, Resources and Exploration and the Northern Territory Geological Survey (NTGS) for providing core samples and advice.

I would like to thank my supervisor Alan Collins for giving me the opportunity to take on this project and the guidance along the way.

I thank Bo Yang for your training on software, equipment and assistance throughout the whole journey.

Thanks you to Robyn Williamson and Tony Hall for their help with clay preparation and processing and Rowan Hansberry for help with clay analysis.

Huge thanks to Sarah Gilbert and David Kelsey from Adelaide microscopy for the polishing, imaging and LA-ICP-MS training.

I cannot forget to thank my family, friends and work colleagues for their support.

REFERENCES

ABBOTT, S. T. & SWEET, I. P. (2000). Tectonic control on third-order sequences in a siliciclastic ramp-style basin: An example from the Roper Superbasin (Mesoproterozoic), northern Australia. *Australian Journal of Earth Sciences* 47(3), 637-657.

ABBOTT, S. T., SWEET, I. P., PLUMB, K. A., YOUNG, D. N., CUTOVINOS, A., FERENCZI, P. A. & PIETSCH, B. A. (2001). Roper Region: Urapunga and Roper River Special, Northern Territory (Second Edition). 1:250 000 geological map series explanatory notes, SD 53-10, 11. *Northern Territory Geological Survey and Geoscience Australia* (National Geoscience Mapping Accord).

AHMAD, M. & MUNSON, T. J. (2013). Northern Territory Geological Survey, Geology and mineral resources of the Northern Territory, Special Publication 5. *Northern Territory Geological Survey*.

BETTS, P. G. & GILES, D. (2006). The 1800–1100 Ma tectonic evolution of Australia. *Precambrian Research* 144(1–2), 92–125.

BETTS, PG, ARMIT, RJ, & AILLERES, L. (2015). Potential-field interpretation mapping of the greater McArthur Basin. PGN Geoscience Report 15/2014. Geophysical and structural interpretation of the greater McArthur Basin. *Northern Territory Geological Survey*, Digital Information Package DIP 015.

BEYER, E. E., HOLLIS, J. A., WHELAN, J. A., GLASS, L. M., DONNELLAN, N., YAXLEY, G., ARMSTRONG, R., ALLEN, C. & SCHERSTÉN, A., (2013). Summary of results. NTGS laser ablation ICPMS and SHRIMP U-Pb, Hf and O geochronology project: Pine Creek Orogen, Arunta Region, Georgina Basin and McArthur Basin, July 2008–May 2011. *Northern Territory Geological Survey*, Record 2012-007.

BEYER, E. E., ALLEN, C. M., ARMSTRONG, R. & WOODHEAD, J. D. (2015). Summary of results. NTGS laser ablation ICPMS U-Pb and Hf geochronology project: selected samples from NAPPERBY 1:250 000 mapsheet area, Arunta Region, July 2010–January 2012. *Northern Territory Geological Survey*, Record 2015-009.

BEYER, E. E., DONNELLAN, N., MEFFRE, S. & THOMPSON, J. M. (2016). Summary of results. NTGS laser ablation ICP-MS in situ zircon and baddeleyite geochronology project: Mount Peake Gabbro, Arunta Region. *Northern Territory Geological Survey*, Record 2016-002.

BIERLEIN, F. P., MAAS, R., & WOODHEAD, J. (2011). Pre-1.8 Ga tectono-magmatic evolution of the Kalkadoon–Leichhardt Belt: implications for the crustal architecture and metallogeny of the Mount Isa Inlier, northwest Queensland, Australia. *Australian Journal of Earth Sciences*, 58(8), 887-915.

BLEWETT, R. S., BLACK, L. P., SUN, S. S., KNUTSON, J., HUTTON, L. J. & BAIN, J. H. C. (1998). U-Pb zircon and Sm-Nd geochronology of the Mesoproterozoic of North Queensland: implications for a Rodinian connection with the Belt supergroup of North America. *Precambrian Research*, 89, 101-127.

BODORKOS, S., BEYER, E. E., EDGOOSE, C. J., WHELAN, J. A., WEBB, G., 639 VANDENBERG, L. C. & HALLETT, L. (2013). Summary of results. Joint NTGS–GA geochronology project: Central and eastern Arunta Region, January 2008 – June 2011. *Northern Territory Geological Survey, Record 2013-003.*

BURNHAM, A, D., BERRY, A, J, . (2017). Formation of Hadean granites by melting of igneous crust. *Nature Geoscience*, 10, 457-462.

CARSON, C. J., CLAOUÉ-LONG, J., STERN, R., CLOSE, D. F., SCRIMGEOUR, I. R. & GLASS, L. M. (2009). Summary of results. Joint NTGS-GA geochronology project: Central and eastern Arunta Region and Pine Creek Orogen, July 2006–May 2007. *Northern Territory Geological Survey*, Record 2009-001.

CHAPPELL, B.W. & WHITE, A. J. R. (1992). I- and S-type granites in the Lachlan Fold Belt. *Trans. R. Soc. Edinb*. 83, 1- 26.

CLAUER, N., WILLIAMS, L.B., FALLICK, A.E. (2014). Genesis of nanometric illite crystals elucidated by light-element (hydrogen, lithium, boron and oxygen) isotope tracing, and K-Ar and Rb-Sr dating. *Chemical Geology.* 383, 26–50.

CLOSE, D. I., BARUCH, E. T., ALTMANN, C. M., COTE, A. J., MOHINUDEEN, F. M., RICHARDS, B. & STONIER, S. 2016. Unconventional gas potential in Proterozoic source rocks: Exploring the Beetaloo Sub-basin. *Northern Territory 'Annual Geoscience exploration Seminar (AGES 2016) Record of abstracts'. Northern Territory Geological Survey*, Record 2016, 91-94.

CLOSE, D. I., COTE, A.J., BARUCH, E.T., ALTMANN, C.M., MOHINUDEEN, F.M., RICHARDS, B., & ILETT, R. (2017). Proterozoic shale gas plays in the Beetaloo Basin and the Amungee NW-1H discovery. *Annual Geoscience Exploration Seminar (AGES Proceedings, Alice Springs, Northern Territory 28–29 March 2017. Northern Territory Geological Survey*, Darwin, 91-97.

COX, G. M., JARRETT, A., EDWARDS, D., CROCKFORD, P. W., HALVERSON, G. P., COLLINS, A. S., ... & LI, Z. X. (2016). Basin redox and primary productivity within the Mesoproterozoic Roper Seaway. *Chemical Geology*, 440, 101-114.

CROSS, A. J., CLAOUÉ-LONG, J. C., SCRIMGEOUR, I. R., CLOSE, D. F. & EDGOOSE, C. J. (2005a). Summary of results. Joint NTGS-GA geochronology project: southern Arunta Region. *Northern Territory Geological Survey*, Record 2004-003.

CROSS, A. J., CLAOUÉ-LONG, J. C., SCRIMGEOUR, I. R., CRISPE, A. & DONNELLAN, N. (2005b). Summary of results. Joint NTGS-GA geochronology project: northern Arunta and Tanami regions, 2000–2003. *Northern Territory Geological Survey*, Record 2005-003.

CROSS, A. J., CLAOUÉ-LONG, J. C., SCRIMGEOUR, I. R., AHMAD, M. & KRUSE, P. D. (2005c). Summary of results. Joint NTGS-GA geochronology project: Rum Jungle, basement to southern Georgina Basin and eastern Arunta Region 2001–2003. *Northern Territory Geological Survey,* Record 2005-006.

CROSS, A. J., PURDY, D. J., BULTITUDE, R. J., BROWN, D. D. & CARR, P. A., (2015). Summary of results. Joint GSQ–GA geochronology project: Thomson Orogen, New England Orogen, Mossman Orogen and Mount Isa region, 2011–2013. *Queensland Geological,* Record 2016/03.

DUNCAN, R. J., WILDE, A. R., BASSANO, K., & MAAS, R. (2006). Geochronological constraints on tourmaline formation in the Western Fold Belt of the Mount Isa Inlier, Australia: Evidence for large-scale metamorphism at 1.57 Ga?. *Precambrian Research*, 146(3), 120-137.

FANNING, C. M. (2012). SHRIMP U-Pb zircon age determinations on detrital zircons from drill core sample ALT-051. ANU Research School of Earth Sciences, PRISE Report 12-260. Esso Australia. *Northern Territory Geological Survey, Core Sampling Report* CSR0211.

FREY, M. (1987). *Low temperature metamorphism*. Blackie and Son.

FREY, M., TEICHMÜLLER, M., TEICHMÜLLER, R., MULLIS, J., KÜNZI, B., BREITSCHMID, A., GRUNER, U.,SCHWIZER, B. (1980). Very low-grade metamorphism in external parts of the Central Alps: illite crystallinity, coal rank and fluid inclusion data. *Eclogae Geol. Helv*, 73, 173–203.

GILES, D., BETTS, P.G., LISTER, G.S. (2002). A continental back-arc setting for Early to Middle Proterozoic basins of northeastern Australia. *Geology*, 30, 823–826.

GORTER, J. D. & GREY, K. (2012). Middle Proterozoic biostratigraphy and log correlations of the Kyalla and Chambers River Formations Beetaloo Sub-basin, Northern Territory, Australia. Central Australian Basins Symposium (CABS) III. Poster. *Petroleum Exploration Society of Australia.*

HANSBERRY, R.L., KING, R.C., COLLINS, A.S.,MORLEY, C.K. (2014). Complex Structure of an Upperlevel Shale Detachment Zone: Khao Khwang Fold and Thrust Belt, Central Thailand. *Structural Geology*, 67, 140–153.

HOLLIS, J.A., BEYER, E. E., WHELAN, J. A., KEMP, A. I. S., SCHERSTÉN, A. & GREIG, A. (2010). Summary of results. NTGS laser U-Pb and Hf geochronology

project: Pine Creek Orogen, Murphy Inlier, McArthur Basin and Arunta Region, July 2007–June 2008. *Northern Territory Geological Survey,* Record 2010-001.

HOLLIS, J. A., CARSON, C. J., GLASS, L. M., KOSITCIN, N., SCHERSTÉN, A., WORDEN, K. E., ARMSTRONG, R. A., YAXLEY, G. M. & KEMP, A. I. S. (2014). Detrital zircon U–Pb–Hf and O isotope character of the Cahill Formation and Nourlangie Schist, Pine Creek Orogen: Implications for the tectonic correlation and evolution of the North Australian Craton. *Precambrian Research,* 246, 35-53.

HOSKIN, P. W. O. & BLACK, L. P. (2000). Metamorphic zircon formation by solid-state recrystallization of protolith igneous zircon. *Journal of metamorphic Geology,* 18(4), 423-439.

JACKSON, M. J., SWEET, I. P., & POWELL, T. G. (1988). Studies on petroleum geology and geochemistry, middle Proterozoic, McArthur Basin Northern Australia I: Petroleum potential. *APEA J,* 28(1), 283-302.

JACKSON, M. J., SWEET, I. P., PAGE, R. W. & BRADSHAW, B. E., (1999). The South Nicholson and Roper Groups: Evidence for the early Mesoproterozoic Roper Superbasin. *In*: Bradshaw B. E. & Scott D. L. eds. *Integrated basin analysis of the Isa Superbasin using seismic, well-log and geopotential data: an evaluation of the economic potential of the northern Lawn Hill Platform. Australian Geological Survey Organisation Record* 1999/19 (CD-ROM), 36-45.

JACKSON, M. J. & SOUTHGATE, P. N. (2000). Evolution of three unconformity-bounded sandy carbonate successions in the McArthur River region of northern Australia: the Lawn, Wide and Doom Supersequences in a proximal part of the Isa Basin. *In*: Cockbain A. E. ed. *Carpentaria-Mt Isa Zinc Belt: basement framework, chronostratigraphy and geodynamic evolution of Proterozoic successions (thematic issue). Australian Journal of Earth Sciences,* 47, 625-635.

JACKSON, S. E., PEARSON, N. J., GRIFFIN, W. L. & BELOUSOVA, E. A. (2004). The application of laser ablation--inductively coupled plasma mass spectrometry to in situ U-Pb zircon geochronology. *Chemical Geology,* 211, 47-69.

KENNEDY, M.J., LÖHR, S.C., FRASER, S.A., BARUCH, E.T. (2014). Direct evidence for organic carbon preservation as clay-organic nanocomposites in a Devonian black shale; from deposition to diagenesis. *Earth Planet. Sci. Lett,* 388, 59–70.

KISCH, H. (1991a). Development of slaty cleavage and degree of very-low-grade metamorphism: a review. J. *Metamorph. Geo,* 9, 735–750.

KISCH, H., FREY, M. (1987). Appendix: Effect of sample preparation on the measured 10 Å peak width of illite (illite-"crystallinity"). Low temperature metamorphism, 301–304.

KOSAKOWSKI, G., KUNERT, V., CLAUSER, C., FRANKE, W., NEUGEBAUER, H.J. (1999). Hydrothermal transients in Variscan crust: paleo-temperature mapping and hydrothermal models. *Tectonophysics*, 306, 325–344.

KOSITCIN, N., CHAMPION, D. C. & HUSTON, D. L. (2009). Geodynamic Synthesis of the North Queensland Region and Implications for Metallogeny. *Geoscience Australia Record, 2009/30,* 196.

KOSITCIN, N., CARSON, C. J., HOLLIS, J. A., GLASS, L. M., CLOSE, D. F., WHELAN, J. A., WEBB, G. & DONNELLAN, N. (2013a). Summary of results. Joint NTGS–GA geochronology project: Arunta Region, Davenport Province and Pine Creek Orogen July 2009 – June 2011. *Northern Territory Geological Survey, Record 2012-008*.

KOSITCIN, N., BEYER, E. E., WHELAN, J. A., CLOSE, D. F., HALLETT, L. & DUNKLEY, D. J. (2013b). Summary of results. Joint NTGS–GA geochronology project: Arunta Region, Ngalia Basin, Tanami Region and Murphy Province, July 2011–June 2012. *Northern Territory Geological Survey, Record, 2013-004*.

KOSITCIN, N., WHELAN, J. A., HALLETT, L. & BEYER, E. E. (2014a). Summary of results. Joint NTGS–GA geochronology project: Amadeus Basin, Arunta Region and Murphy Province, July 2012–June 2013. *Northern Territory Geological Survey, Record 2014-005*.

KOSITCIN, N., BEYER, E. E. & WHELAN, J. A. (2014b). Summary of results. Joint NTGS–GA SHRIMP geochronology project: Arunta Region, July 2013–June 2014. *Northern Territory Geological Survey, Record 2014-008*.

KOSITCIN, N., KRAUS, S. & WHELAN, J. A. (2015a). Summary of results. Joint NTGS–GA SHRIMP geochronology project: Arnhem Province, July 2014–June 2015. *Northern Territory Geological Survey, Record 2015-010.*

KOSITCIN, N., RENO, B. L. & WHELAN, J. A. (2015b). Summary of results. Joint NTGS–GA geochronology project: Arunta Region, July 2014–June 2015. *Northern Territory Geological Survey, Record 2015-007*.

KÜBLER, B. (1968). Evaluation quantitative du metamorphism par la cristallinite de l'Illite. Bull. *Centre Rech. Pau* SNPA 2, 385–397.

KÜBLER, B., JABOYEDOFF, M. (2000). Illite crystallinity: Comptes Rendus de l'Académie des Sciences-Series IIA. *Earth Planet. Sci*, 331, 75–89.

LINDGREEN, H., DRITS, V.A., SAKHAROV, B.A., SALYN, A.L., WRANG, P., DAINYAK, L.G. (2000). Illitesmectite structural changes during metamorphism in black Cambrian Alum shales from the Baltic area. *Am. Mineral*, 85, 1223–1238.

MÄHLMANN, R.F., BOZKAYA, Ö., POTEL, S., LE BAYON, R., ŠEGVIĆ, B., NIETO, F. (2012). The pioneer work of Bernard Kübler and Martin Frey in very

low-grade metamorphic terranes: paleo-geothermal potential of variation in Kübler-Index/organic matter reflectance correlations. *A review. Swiss J. Geosci*, 105, 121–152.

MUNSON, T. J. (2016). Sedimentary characterisation of theWilton package, greater McArthur Basin. Northern Territory. 'Annual Geoscience exploration Seminar (AGES 2016) Record of abstracts'. Northern Territory Geological Survey, Record 2016, 84-89.

NEUMANN, N. L., GIBSON, G. M. & SOUTHGATE, P. N. (2009). New SHRIMP age constraints on the timing and duration of magmatism and sedimentation in the Mary Kathleen Fold Belt, Mt Isa Inlier, Australia. Australian Journal of Earth Sciences 56(7), 965-983.

NEUMANN, N. L., SOUTHGATE, P. N., GIBSON, G. M. & MCINTYRE, A. (2006). New SHRIMP geochronology for the Western Fold Belt of the Mt Isa Inlier: developing a 1800 – 1650 Ma event framework. Australian Journal of Earth Sciences 53(6), 1023-1039.

PAGE, R. W. & SUN, S.-S. (1998). Aspects of geochronology and crustal evolution in the Eastern Fold Belt, Mt Isa Inlier. Australian Journal of Earth Sciences 45(3), 343-361.

PATON, C., HELLSTROM, J., PAUL, B., WOODHEAD, J., & HERGT, J. (2011). Iolite: Freeware for the visualisation and processing of mass spectrometric data. Journal of Analytical Atomic Spectrometry, 26(12), 2508-2518.

RAWLINGS, D.J. (1999). Stratigraphic resolution of a multiphase intracratonic basin system: The McArthur Basin, northern Australia. Australian Journal of Earth Sciences, 46(5), 703-723.

RAWLINGS, D.J., Korsch, R. J., Goleby, B. R., Gibson, G. M., Johnstone, D. W., & Barlow, M. (2004). The 2002 southern McArthur Basin seismic reflection survey. Geoscience Australia Record, 17, 78.

Rawlings DJ, Sweet IP and Kruse PD, (2008). Mount Drummond, Northern Territory. 1:250 000 geological map series explanatory notes, SE 53-12. Northern Territory Geological Survey, Darwin.

REVIE, D. (2016). From the back of the shed to the forefront of exploration: what the NTGS core store is revealing about the Roper Group shales of the greater McArthur Basin. 'Annual Geoscience Exploration Seminar (AGES) Proceedings, Alice Springs, Northern Territory 15–16 March 2016'. *Northern Territory Geological Survey, Darwin.*

REVIE, D. (2017).Volumetric resource assessment of the lower Kyalla and middle Velkerri formations of the McArthur Basin. Annual Geoscience Exploration Seminar

(AGES) Proceedings, Alice Springs, Northern Territory 28–29 March 2017. *Northern Territory Geological Survey, Darwin*, 86-90.

SLAMA, J., KOSLER, J., CONDON, D. J., CROWLEY, J. L., GERDES, A., HANCHAR, J. M., SCHALTEGGER, U. (2008). Plešovice zircon—a new natural reference material for U–Pb and Hf isotopic microanalysis. Chemical Geology, 249(1), 1-35.

SPENCER, C. J., & KIRKLAND, C. L. (2016). Visualizing the sedimentary response through the orogenic cycle: A multidimensional scaling approach. *Lithosphere*, 8(1), 29-37.

TAYLOR, S. R., MCLENNAN, S. M. (1985) The continental crust: its composition and evolution. Blackwell, Oxford.

UNDERWOOD, M.B., LAUGHLAND, M.M., KANG, S.M. (1993). A comparison among organic and inorganic indicators of diagenesis and low-temperature metamorphism. Thermal evolution of the Tertiary Shimanto Belt, Southwest Japan: An example of Ridge-Trench interaction. *GSA Special Paper*, 273, 45.

VERMEESCH, P. (2013). Multi-sample comparison of detrital age distributions. *Chemical Geology*, 341, 140-146.

VERMEESCH, P. (2014). Corrigendum to "Multi-sample comparison of detrital age distributions" [*Chem. Geol.* 341 (11 March 2013)—140-146]. *Chemical Geology*, 380, 191.

WADE, B. P. (2006). *Unravelling the tectonic framework of the Musgrave Province, central Australia*. PhD Thesis. University of Adelaide.

WARR, L., RICE, A. (1994). Interlaboratory standardization and calibration of day mineral crystallinity and crystallite size data. J. *Metamorph. Geol*. 12, 141–152.

WARR, L.N., GREILING, R.O., ZACHRISSON, E. (1996). Thrust-related very low grade metamorphism in the marginal part of an orogenic wedge, Scandanavian Caledonides. *Tectonics*, 15 (6), 1213-1229.

WORDEN, K. E., CLAOUÉ-LONG, J. C., SCRMGEOUR, I. R. & DOYLE, N. (2006a). Summary of results. Joint NTGS-GA geochronology project: Pine Creek Orogen and Arunta Region, January– June 2004. *Northern Territory Geological Survey*, Record 2006-005.

WORDEN, K. E., CLAOUÉ-LONG, J. C. & SCRIMGEOUR, I. R. (2006b). Summary of results. Joint NTGS-GA geochronology project: Pine Creek Orogen, Tanami Region, Arunta Region and Amadeus Basin, July–December 2004. *Northern Territory Geological Survey*, Record 2006-006.

WORDEN, K. E., CARSOU, C. J., CLOSE, D. F., DONNELLAN, N. & SCRIMGEOUR, I. R. (2008). Summary of results. Joint NTGS-GA geochronology project: Tanami Region, Arunta Region, Pine Creek Orogen and Halls Creek January 2005–March 2007. *Northern Territory Geological Survey*, Record 2008-003.

YANG, B. et al. in review. Spatial and temporal detrital zircon U-Pb provenance of the hydrocarbon-bearing upper Roper Group, Beetaloo Sub-basin, Northern Territory, Australia.

APPENDIX A: ALL CONCORDANT ZIRCON AGE DATA

Altree AN2 - Velkerri Formation (Upper)										
	Final 207_235	Final 207_235 _Int2SE	Final206_ 238	Final206_238 _Int2SE	Error Correlation _6_38vs7_35	FinalAge206 _238	FinalAge206_238_Int 2SE	FinalAge207_206	FinalAge207_206_Int2SE	Conc (%)
1	3.474	0.078	0.2547	0.0065	0.62621	1461	33	1598	46	91
2	3.93	0.18	0.2698	0.0093	0.49031	1538	47	1617	73	95
3	3.66	0.12	0.2663	0.009	0.84662	1520	46	1652	33	92
4	4.868	0.095	0.3117	0.0077	0.68482	1747	38	1853	31	94

Altree AN3- Velkerri Formation (Lower)										
	Final 207_235	Final 207_235 _Int2SE	Final206_ 238	Final206_238 _Int2SE	Error Correlation _6_38vs7_35	FinalAge206 _238	FinalAge206_238_Int 2SE	FinalAge207_206	FinalAge207_206_Int2SE	Conc (%)
1	2.87	0.12	0.2307	0.0079	0.71687	1338	41	1459	55	92
2	2.92	0.15	0.226	0.0087	0.25038	1322	49	1459	70	91
3	3.156	0.082	0.2496	0.0071	0.86467	1435	37	1466	25	98
4	3.161	0.081	0.2511	0.008	0.58871	1442	42	1468	53	98
5	3.18	0.14	0.2529	0.0072	0.47115	1452	37	1481	74	98
6	3.418	0.077	0.2714	0.0062	0.64011	1547	32	1484	37	104
7	3.53	0.12	0.2746	0.0084	0.50784	1562	42	1501	62	104
8	3.39	0.15	0.262	0.01	0.24527	1503	54	1510	100	100
9	3.23	0.11	0.254	0.011	0.84163	1459	56	1514	40	96
10	3.43	0.11	0.268	0.0078	0.43416	1540	39	1528	61	101
11	3.85	0.14	0.297	0.012	0.67363	1672	57	1529	58	109
12	3.81	0.11	0.287	0.01	0.61762	1623	51	1547	58	105
13	3.43	0.13	0.2561	0.0071	0.57488	1468	36	1553	62	95

14	3.526	0.088	0.2619	0.0074	0.61952	1498	38	1564	45	96
15	3.99	0.11	0.2997	0.007	0.72853	1688	35	1577	35	107
16	3.633	0.066	0.2684	0.0052	0.48425	1536	27	1577	33	97
17	3.44	0.14	0.2652	0.0073	0.62488	1521	36	1580	57	96
18	3.64	0.11	0.2634	0.0055	0.32634	1506	28	1589	59	95
19	3.53	0.16	0.261	0.016	0.79973	1495	81	1591	72	94
20	3.87	0.1	0.2843	0.007	0.33882	1611	35	1593	48	101
21	3.613	0.087	0.2669	0.0089	0.7869	1523	45	1596	37	95
22	3.597	0.08	0.2669	0.0068	0.70338	1524	35	1598	33	95
23	3.867	0.067	0.2835	0.0053	0.59021	1608	27	1605	30	100
24	4.045	0.081	0.2913	0.0066	0.64992	1646	33	1617	34	102
25	4.21	0.11	0.3012	0.0077	0.29599	1696	38	1619	63	105
26	4.27	0.13	0.3073	0.0084	0.4123	1725	42	1632	63	106
27	3.672	0.094	0.2679	0.0065	0.59109	1529	33	1643	37	93
28	3.64	0.13	0.2634	0.0087	0.56184	1506	45	1644	58	92
29	4.1	0.14	0.2911	0.008	0.41632	1646	40	1646	65	100
30	3.97	0.11	0.2846	0.0066	0.69441	1613	33	1646	36	98
31	4.09	0.19	0.2894	0.0081	0.42358	1637	41	1669	79	98
32	3.86	0.13	0.2689	0.0071	0.46146	1534	36	1670	54	92
33	4.291	0.077	0.3007	0.0064	0.70881	1693	32	1674	27	101
34	4.05	0.13	0.286	0.01	0.73057	1620	52	1675	44	97
35	4.25	0.12	0.3003	0.0063	0.56173	1695	31	1676	42	101
36	4.19	0.12	0.2928	0.0074	0.42604	1654	37	1677	42	99
37	4.06	0.1	0.2902	0.0074	0.67871	1647	35	1680	35	98
38	4.06	0.14	0.291	0.008	0.63556	1646	40	1682	52	98
39	4.05	0.15	0.29	0.01	0.61306	1638	51	1688	40	97
40	3.87	0.19	0.271	0.014	0.51188	1543	71	1688	96	91
41	4.25	0.15	0.2916	0.009	0.28313	1647	45	1692	72	97
42	4.243	0.097	0.2998	0.007	0.63206	1689	34	1692	39	100

43	3.93	0.13	0.2761	0.0082	0.6533	1570	41	1699	50	92
44	4.01	0.17	0.275	0.0086	0.36992	1565	43	1701	81	92
45	4.66	0.14	0.3261	0.0098	0.70602	1817	48	1708	50	106
46	4.42	0.12	0.3052	0.008	0.61147	1724	39	1709	41	101
47	4.36	0.1	0.3012	0.0086	0.51224	1695	43	1717	44	99
48	3.95	0.12	0.2749	0.0086	0.80463	1564	44	1718	32	91
49	4.371	0.081	0.3006	0.0059	0.68198	1693	29	1719	30	98
50	4.25	0.12	0.2968	0.007	0.17741	1674	35	1721	64	97
51	4.55	0.15	0.3099	0.0074	0.60103	1739	37	1724	44	101
52	4.62	0.15	0.3126	0.0097	0.84501	1751	48	1725	38	102
53	4.14	0.28	0.281	0.017	0.4136	1594	84	1726	84	92
54	4.05	0.12	0.2769	0.0091	0.54352	1575	46	1731	54	91
55	4.28	0.11	0.2932	0.0078	0.74532	1656	39	1731	31	96
56	4.7	0.13	0.3215	0.0077	0.55009	1795	38	1740	46	103
57	4.2	0.098	0.2859	0.0083	0.79416	1619	42	1742	33	93
58	4.61	0.12	0.3128	0.0077	0.72748	1757	38	1744	33	101
59	4.42	0.11	0.3002	0.0079	0.8139	1691	39	1748	29	97
60	4.502	0.099	0.3067	0.0078	0.81732	1727	38	1749	21	99
61	4.44	0.11	0.2968	0.0061	0.49306	1679	31	1751	41	96
62	4.905	0.099	0.3343	0.007	0.62333	1858	34	1752	36	106
63	4.3	0.1	0.287	0.01	0.58018	1626	52	1754	48	93
64	4.32	0.14	0.2881	0.0094	0.68044	1631	47	1756	57	93
65	4.99	0.11	0.332	0.0081	0.73754	1851	38	1756	31	105
66	4.522	0.096	0.3048	0.0075	0.76946	1713	37	1759	29	97
67	4.55	0.17	0.3012	0.0083	0.19395	1701	40	1760	63	97
68	4.63	0.21	0.3089	0.0089	0.18776	1746	44	1760	63	99
69	4.4	0.11	0.3028	0.0093	0.77672	1703	46	1762	36	97
70	5.1	0.14	0.343	0.011	0.73677	1899	51	1770	35	107
71	4.539	0.087	0.3065	0.0068	0.77906	1722	34	1770	24	97

72	5.16	0.11	0.3436	0.009	0.83233	1902	43	1778	25	107
73	4.56	0.14	0.309	0.011	0.70054	1733	55	1778	51	97
74	4.4	0.13	0.2938	0.0086	0.77721	1658	43	1778	36	93
75	4.52	0.15	0.3014	0.0084	0.7097	1697	42	1780	47	95
76	4.26	0.15	0.2846	0.0089	0.8321	1613	45	1781	34	91
77	4.7	0.13	0.3157	0.0069	0.64318	1767	34	1782	41	99
78	4.28	0.15	0.289	0.0068	0.73551	1636	34	1782	39	92
79	4.67	0.14	0.314	0.011	0.73692	1760	54	1783	45	99
80	4.66	0.16	0.3122	0.0073	0.34109	1750	36	1784	64	98
81	4.74	0.14	0.3202	0.0091	0.76926	1788	45	1786	33	100
82	5.22	0.14	0.3472	0.0091	0.79523	1919	44	1791	38	107
83	4.86	0.11	0.3195	0.0097	0.7453	1785	48	1792	39	100
84	4.3	0.17	0.289	0.013	0.74961	1636	66	1793	49	91
85	4.81	0.096	0.3158	0.0073	0.60625	1768	36	1804	35	98
86	5.18	0.17	0.3453	0.0099	0.57456	1910	48	1805	51	106
87	4.64	0.11	0.31	0.0074	0.6928	1739	36	1807	31	96
88	4.91	0.13	0.3247	0.0085	0.76322	1811	42	1807	39	100
89	5.31	0.18	0.3403	0.0077	0.65586	1887	37	1819	45	104
90	5.12	0.13	0.3303	0.0083	0.66905	1838	40	1823	32	101
91	4.55	0.18	0.2993	0.0096	0.72674	1686	48	1826	50	92
92	5.11	0.11	0.3287	0.0081	0.71314	1834	40	1835	35	100
93	4.87	0.1	0.3186	0.0072	0.68509	1782	35	1841	27	97
94	4.81	0.1	0.3042	0.0089	0.76434	1711	44	1860	32	92
95	5.16	0.14	0.331	0.007	0.62233	1842	34	1862	37	99
96	5.03	0.11	0.3284	0.0083	0.66195	1828	40	1863	35	98
97	4.94	0.19	0.307	0.017	0.67833	1722	85	1882	80	91
98	5.31	0.17	0.33	0.011	0.75997	1838	55	1884	51	98
99	5.05	0.14	0.3125	0.0081	0.75822	1757	41	1903	33	92
100	5.14	0.17	0.3214	0.0089	0.40378	1800	42	1908	62	94

101	5.7	1	0.35	0.052	0.82395	1890	240	1920	160	98
102	7.22	0.21	0.392	0.01	0.88295	2134	48	2125	25	100
103	10.55	0.32	0.463	0.014	0.85481	2450	63	2524	29	97
104	9.8	0.28	0.429	0.016	0.77831	2297	73	2538	35	91
105	13.1	0.4	0.54	0.016	0.74693	2781	69	2617	37	106
106	19.09	0.38	0.577	0.013	0.82578	2935	52	3112	21	94

Altree ALT09 - Corcoran Formation

	Final 207_235	Final 207_235 _Int2SE	Final206_ 238	Final206_238 _Int2SE	Error Correlation _6_38vs7_35	FinalAge206 _238	FinalAge206_238_Int 2SE	FinalAge207_206	FinalAge207_206_Int2SE	Concordance (%)
1	2.62	0.14	0.219	0.011	0.74353	1288	59	1375	67	94
2	2.717	0.061	0.2255	0.0056	0.35605	1311	29	1387	48	95
3	2.996	0.078	0.2395	0.0036	0.62529	1384	19	1420	37	97
4	3.22	0.13	0.2593	0.0056	0.21469	1485	29	1423	74	104
5	2.89	0.14	0.2308	0.0098	0.69141	1338	52	1426	62	94
6	3.19	0.1	0.2536	0.0052	0.27843	1456	27	1429	66	102
7	2.86	0.3	0.2256	0.0098	0.53689	1311	51	1430	150	92
8	3.219	0.081	0.2582	0.0038	0.59857	1480	20	1431	39	103
9	3.092	0.074	0.2479	0.0048	0.40453	1427	25	1433	47	100
10	3.282	0.055	0.2608	0.0058	0.7215	1500	30	1435	27	105
11	3.111	0.073	0.2493	0.0054	0.32389	1434	28	1448	47	99
12	3.41	0.14	0.2696	0.0049	0.39537	1538	25	1453	76	106
13	3.131	0.085	0.2496	0.0064	0.29644	1435	33	1453	55	99
14	3.18	0.14	0.251	0.011	0.67944	1444	59	1454	68	99
15	3.24	0.099	0.2576	0.0067	0.53926	1476	34	1462	54	101
16	3.185	0.08	0.2536	0.0064	0.65494	1455	33	1463	40	99

17	2.987	0.08	0.2348	0.005	0.56631	1359	26	1466	41	93
18	3.04	0.11	0.2367	0.0065	0.68748	1369	34	1468	46	93
19	3.262	0.098	0.256	0.0049	0.64078	1469	25	1469	43	100
20	3.43	0.11	0.271	0.0066	0.20376	1545	33	1469	69	105
21	3.221	0.095	0.2631	0.0051	0.38329	1505	26	1475	62	102
22	3.11	0.11	0.2468	0.0073	0.66225	1421	38	1479	60	96
23	3.159	0.072	0.2512	0.0069	0.67378	1444	35	1490	37	97
24	3.27	0.11	0.2579	0.0047	0.093	1478	24	1492	71	99
25	3.16	0.11	0.2439	0.0075	0.68452	1406	39	1507	45	93
26	3.136	0.092	0.2441	0.0069	0.64829	1407	36	1509	38	93
27	3.25	0.17	0.2561	0.0075	0.089707	1469	38	1510	110	97
28	3.341	0.098	0.2578	0.0079	0.35663	1485	38	1515	62	98
29	3.19	0.11	0.2466	0.006	0.56545	1420	31	1524	51	93
30	3.19	0.083	0.2446	0.0074	0.63347	1409	38	1526	49	92
31	3.46	0.12	0.2672	0.0074	0.87685	1525	38	1528	28	100
32	3.29	0.15	0.2469	0.0088	0.72537	1422	46	1528	61	93
33	3.567	0.074	0.2725	0.0058	0.74535	1552	30	1529	32	102
34	3.25	0.12	0.2463	0.0044	0.29901	1419	23	1531	69	93
35	3.38	0.17	0.2646	0.0059	0.42097	1512	30	1536	79	98
36	3.33	0.11	0.2504	0.0068	0.63967	1440	35	1546	46	93
37	3.78	0.13	0.2821	0.0072	0.34821	1606	35	1548	67	104
38	3.548	0.091	0.2674	0.0054	0.64188	1527	28	1549	34	99
39	3.813	0.086	0.2862	0.0053	0.47759	1625	27	1552	37	105
40	3.63	0.14	0.2686	0.0053	0.31406	1536	26	1554	68	99
41	3.49	0.11	0.2626	0.0067	0.6069	1503	34	1554	58	97
42	3.54	0.067	0.2667	0.0044	0.55172	1523	23	1557	34	98
43	3.333	0.095	0.2449	0.007	0.69494	1411	36	1561	47	90
44	3.786	0.083	0.2808	0.0054	0.62376	1594	27	1569	34	102
45	3.892	0.074	0.2912	0.0046	0.59438	1647	23	1575	30	105

46	3.75	0.12	0.2742	0.0054	0.27673	1561	28	1579	58	99
47	3.58	0.12	0.2656	0.008	0.70749	1517	41	1580	47	96
48	3.582	0.092	0.2624	0.0068	0.7646	1500	35	1582	33	95
49	3.769	0.099	0.279	0.0052	0.32024	1585	26	1587	49	100
50	3.709	0.086	0.2733	0.0062	0.71804	1561	32	1588	34	98
51	3.79	0.11	0.2757	0.0067	0.39244	1569	34	1589	52	99
52	3.74	0.11	0.274	0.0077	0.67141	1560	39	1594	43	98
53	3.87	0.15	0.2829	0.0089	0.52886	1610	44	1596	60	101
54	3.814	0.075	0.2818	0.0064	0.71597	1599	32	1598	32	100
55	3.77	0.091	0.2796	0.0061	0.45108	1592	31	1598	44	100
56	3.95	0.14	0.2882	0.0052	0.31147	1635	26	1603	63	102
57	3.879	0.08	0.2846	0.0044	0.54389	1614	22	1610	34	100
58	3.77	0.16	0.2798	0.0077	0.30281	1588	39	1615	74	98
59	3.59	0.09	0.2605	0.0047	0.53788	1492	24	1617	39	92
60	3.923	0.079	0.2854	0.006	0.54102	1617	30	1620	37	100
61	3.97	0.1	0.2919	0.0062	0.60912	1650	31	1622	42	102
62	3.972	0.082	0.2877	0.0051	0.50226	1629	26	1626	32	100
63	3.709	0.085	0.2714	0.0062	0.62918	1547	32	1628	37	95
64	4.08	0.11	0.2982	0.0054	0.44192	1681	27	1632	45	103
65	4.013	0.071	0.2886	0.0047	0.51364	1634	24	1634	32	100
66	3.95	0.12	0.287	0.0062	0.35966	1625	31	1637	57	99
67	4.27	0.2	0.309	0.011	0.13019	1732	54	1638	93	106
68	4.05	0.13	0.2869	0.0073	0.45682	1624	36	1642	51	99
69	4.34	0.12	0.3082	0.0077	0.43484	1731	38	1657	47	104
70	4.14	0.16	0.296	0.011	0.83825	1667	55	1673	44	100
71	4.34	0.16	0.3022	0.007	0.57244	1700	35	1691	59	101
72	4.274	0.097	0.2988	0.0075	0.76296	1683	37	1698	29	99
73	4.86	0.11	0.3331	0.0077	0.59987	1852	37	1706	36	109
74	4.48	0.1	0.3103	0.006	0.37794	1745	29	1709	46	102

75	4.67	0.12	0.3216	0.0059	0.54512	1797	29	1711	39	105
76	4.34	0.12	0.3016	0.0077	0.32169	1698	38	1713	51	99
77	4.54	0.12	0.316	0.0062	0.24101	1774	31	1714	57	104
78	4.6	0.13	0.3184	0.0051	0.44569	1781	25	1715	49	104
79	4.59	0.14	0.3096	0.0088	0.37902	1736	44	1725	59	101
80	4.85	0.15	0.3291	0.0065	0.41026	1833	31	1726	54	106
81	4.23	0.085	0.2894	0.0067	0.74696	1637	33	1734	25	94
82	4.64	0.087	0.3141	0.0044	0.50148	1760	22	1737	32	101
83	4.58	0.18	0.309	0.0069	0.012559	1735	34	1741	81	100
84	4.48	0.11	0.3086	0.0073	0.73384	1732	36	1741	29	99
85	4.759	0.085	0.3192	0.0061	0.54456	1785	30	1743	30	102
86	4.62	0.15	0.312	0.011	0.31608	1751	54	1743	48	100
87	4.91	0.12	0.3227	0.0057	0.41558	1802	28	1749	41	103
88	4.229	0.073	0.2888	0.0063	0.61982	1634	31	1756	32	93
89	4.71	0.13	0.321	0.011	0.46216	1791	56	1756	55	102
90	4.62	0.1	0.311	0.0075	0.60065	1743	37	1769	34	99
91	5.15	0.18	0.341	0.013	0.42263	1890	62	1771	79	107
92	4.79	0.17	0.3175	0.0075	0.56095	1776	37	1773	55	100
93	4.85	0.11	0.3273	0.0084	0.66029	1824	41	1781	31	102
94	4.93	0.1	0.3245	0.0065	0.66034	1811	32	1800	28	101
95	4.54	0.2	0.3024	0.0073	0.48721	1708	37	1800	71	95
96	5.23	0.12	0.3394	0.0077	0.61715	1882	37	1807	37	104
97	4.94	0.059	0.3246	0.0044	0.50307	1812	21	1816	24	100
98	4.87	0.15	0.3172	0.0071	0.52192	1775	35	1819	44	98
99	5.19	0.099	0.3345	0.0064	0.64375	1859	31	1821	27	102
100	5.013	0.094	0.3246	0.0072	0.73823	1815	34	1824	24	100
101	5.27	0.12	0.3374	0.0083	0.64689	1872	40	1829	35	102
102	4.88	0.14	0.3187	0.0081	0.50197	1782	39	1832	49	97
103	5.066	0.091	0.3269	0.0066	0.54621	1825	32	1833	35	100

104	4.6	0.22	0.293	0.0078	0.38854	1656	39	1833	86	90
105	5.14	0.12	0.3309	0.0064	0.3344	1841	31	1834	45	100
106	5.28	0.15	0.3416	0.0083	0.63186	1893	40	1840	36	103
107	5.1	0.18	0.3313	0.0069	0.29306	1844	33	1856	65	99
108	5.62	0.11	0.3544	0.0051	0.56795	1955	24	1875	30	104
109	5.25	0.12	0.3329	0.0079	0.63921	1851	38	1876	37	99
110	5.6	0.12	0.3468	0.0073	0.57103	1918	35	1877	35	102
111	5.44	0.083	0.3449	0.0072	0.76323	1909	35	1890	24	101
112	5.01	0.14	0.313	0.0077	0.61935	1754	38	1915	39	92
113	9.61	0.19	0.4672	0.0067	0.44302	2471	30	2342	35	106
114	11.44	0.2	0.4991	0.0086	0.60374	2608	37	2542	25	103
115	12.28	0.46	0.511	0.017	0.91712	2652	73	2603	26	102
116	14.13	0.33	0.551	0.013	0.82954	2823	53	2702	24	104

	Jamison JN5 - Kyalla Formation									
	Final 207_235	Final 207_235 _Int2SE	Final206_ 238	Final206_238 _Int2SE	Error Correlation _6_38vs7_35	FinalAge206 _238	FinalAge206_238_Int 2SE	FinalAge20 7_206	FinalAge207_206_Int2SE	Concordance (%)
1	3.543	0.063	0.268	0.0058	0.5824	1533	29	1562	30	98
2	3.5	0.12	0.2685	0.0058	0.51409	1532	29	1565	45	98
3	3.61	0.1	0.2628	0.006	0.70785	1503	30	1588	33	95
4	3.86	0.12	0.2828	0.0075	0.5121	1603	38	1590	51	101
5	4.03	0.14	0.29	0.01	0.59472	1641	52	1597	58	103
6	4.14	0.15	0.3042	0.0091	0.53621	1718	47	1607	51	107
7	4.2	0.11	0.3051	0.0075	0.81536	1715	37	1608	27	107
8	4.28	0.12	0.3011	0.009	0.48967	1695	45	1641	58	103
9	4.18	0.11	0.2952	0.0079	0.67137	1671	40	1656	35	101

10	4.27	0.11	0.2986	0.0077	0.49175	1683	38	1677	49	100
11	4.32	0.18	0.2979	0.009	0.18581	1679	45	1697	90	99
12	4.43	0.12	0.3017	0.0077	0.6222	1698	38	1704	37	100
13	4.03	0.17	0.2842	0.0087	0.25425	1611	44	1709	81	94
14	4.5	0.093	0.3014	0.0068	0.66661	1707	36	1712	31	100
15	4.42	0.14	0.3047	0.008	0.50392	1713	40	1713	48	100
16	4.35	0.17	0.291	0.01	0.62068	1647	50	1717	62	96
17	4.589	0.084	0.3132	0.0058	0.46074	1755	29	1737	33	101
18	4.62	0.17	0.3108	0.0087	0.49303	1743	43	1744	52	100
19	4.33	0.12	0.2881	0.0065	0.45814	1631	33	1746	49	93
20	4.27	0.25	0.291	0.017	0.55845	1641	83	1750	110	94
21	4.788	0.096	0.3185	0.0065	0.61737	1781	32	1753	27	102
22	4.8	0.11	0.3185	0.0068	0.58011	1785	34	1768	34	101
23	4.3	0.12	0.2941	0.0063	0.64663	1661	31	1769	43	94
24	4.65	0.13	0.3026	0.0082	0.39456	1703	40	1779	53	96
25	4.4	0.11	0.2944	0.0092	0.77755	1661	46	1788	41	93
26	4.64	0.13	0.3006	0.0091	0.58369	1692	45	1788	38	95
27	4.985	0.095	0.3328	0.0063	0.6128	1851	30	1789	31	103
28	4.95	0.13	0.3228	0.0081	0.70796	1802	39	1796	34	100
29	4.87	0.16	0.322	0.0098	0.0067411	1797	48	1802	56	100
30	4.76	0.14	0.3122	0.009	0.7394	1750	44	1804	37	97
31	4.39	0.16	0.2939	0.0093	0.64489	1660	46	1804	46	92
32	4.9	0.15	0.3226	0.0092	0.78026	1800	45	1816	37	99
33	4.61	0.16	0.302	0.011	0.74362	1700	56	1818	48	94
34	4.84	0.17	0.311	0.01	0.67396	1752	52	1840	50	95
35	5.21	0.1	0.3305	0.0083	0.62712	1839	40	1849	31	99
36	5.18	0.28	0.323	0.012	0.25081	1807	61	1850	96	98
37	5.35	0.13	0.3315	0.0091	0.68371	1844	44	1880	37	98
38	5.08	0.33	0.313	0.012	0.31526	1752	61	1880	110	93

39	5.46	0.15	0.3411	0.0095	0.55829	1891	46	1919	45	99
40	5.31	0.25	0.32	0.017	0.5935	1785	81	1954	86	91
41	6.09	0.14	0.3459	0.0086	0.66503	1920	40	2006	35	96
42	8.25	0.16	0.4134	0.0082	0.65517	2235	36	2313	27	97
43	8.5	0.45	0.398	0.018	0.46977	2159	83	2343	64	92
44	9.71	0.33	0.437	0.017	0.55065	2334	77	2495	61	94
45	10.36	0.37	0.456	0.015	0.83806	2422	68	2525	35	96

Jamison JN6 - Kyalla Formation										
	Final 207_235	Final 207_235 _Int2SE	Final206_ 238	Final206_238 _Int2SE	Error Correlation _6_38vs7_35	FinalAge206 _238	FinalAge206_238_Int 2SE	FinalAge20 7_206	FinalAge207_206_Int2SE	Concordance (%)
1	3.06	0.26	0.242	0.017	0.5177	1394	86	1420	120	98
2	2.93	0.18	0.233	0.01	0.63916	1351	54	1428	63	95
3	3.98	0.14	0.298	0.01	0.26815	1681	50	1647	72	102
4	3.84	0.14	0.275	0.0076	0.45086	1565	38	1653	61	95
5	3.85	0.16	0.281	0.01	0.43224	1596	52	1663	84	96
6	4.04	0.14	0.279	0.0071	0.69232	1586	36	1671	47	95
7	4.38	0.17	0.2947	0.009	0.61022	1663	45	1699	67	98
8	4.55	0.1	0.3093	0.006	0.5064	1736	29	1702	38	102
9	4.26	0.12	0.3001	0.0088	0.52296	1690	44	1710	53	99
10	4.47	0.15	0.28	0.01	0.62996	1588	51	1712	47	93
11	4.15	0.19	0.286	0.01	0.75642	1622	52	1718	56	94
12	4.31	0.1	0.2914	0.0078	0.59215	1647	39	1718	34	96
13	4.16	0.18	0.294	0.013	0.64024	1661	64	1719	62	97
14	4.17	0.13	0.2857	0.0065	0.42774	1619	33	1724	56	94
15	4.11	0.17	0.2833	0.0068	0.36485	1607	34	1727	73	93

16	4.12	0.15	0.2924	0.0074	0.41878	1652	37	1737	55	95
17	4.28	0.19	0.287	0.01	0.76775	1628	51	1740	49	94
18	4.37	0.15	0.3028	0.0094	0.43711	1704	47	1742	51	98
19	4.91	0.16	0.323	0.01	0.6407	1805	49	1745	47	103
20	4.2	0.24	0.289	0.01	0.42549	1635	51	1748	96	94
21	4.52	0.1	0.3028	0.0077	0.66305	1703	38	1749	38	97
22	4.44	0.27	0.293	0.012	0.40471	1655	59	1750	110	95
23	4.3	0.13	0.2907	0.0073	0.50126	1644	37	1753	55	94
24	4.32	0.18	0.2989	0.0096	0.14576	1683	48	1766	81	95
25	4.56	0.12	0.3038	0.0078	0.65131	1709	39	1768	39	97
26	4.311	0.099	0.2956	0.0046	0.40769	1669	23	1775	33	94
27	4.44	0.23	0.294	0.015	0.17473	1658	75	1792	74	93
28	5.14	0.14	0.302	0.01	0.63347	1698	51	1794	49	95
29	4.72	0.28	0.316	0.014	0.6351	1765	69	1795	87	98
30	4.596	0.097	0.3114	0.0079	0.46221	1746	39	1804	43	97
31	5.048	0.094	0.3301	0.0049	0.51468	1838	24	1811	30	101
32	4.91	0.11	0.3034	0.0093	0.47317	1706	46	1811	52	94
33	4.56	0.11	0.3068	0.009	0.60858	1724	44	1813	40	95
34	5.26	0.16	0.3516	0.0081	0.59752	1941	39	1847	43	105
35	4.99	0.14	0.3136	0.008	0.57491	1757	39	1883	40	93

Jamison JN1 - Bukalara Formation

	Final 207_235	Final 207_235 _Int2SE	Final206_ 238	Final206_238 _Int2SE	Error Correlation _6_38vs7_35	FinalA ge206 _238	FinalAge20 6_238_Int 2SE	FinalAge20 7_206	FinalAge207_2 06_Int2SE	Concordance (%)
1	2.83	0.12	0.2323	0.0079	0.47794	1346	41	1357	58	99
2	3.7	0.15	0.2728	0.0064	0.16277	1559	32	1560	30	100

3	3.9	0.15	0.2898	0.0089	0.34855	1638	45	1577	81	104
4	3.41	0.15	0.2535	0.006	0.33134	1456	31	1591	89	92
5	3.82	0.12	0.275	0.0067	0.18341	1570	33	1621	42	97
6	3.78	0.15	0.276	0.012	0.49335	1568	60	1623	29	97
7	3.69	0.12	0.265	0.0082	0.67306	1514	42	1624	76	93
8	3.97	0.13	0.2766	0.0074	0.33093	1573	37	1626	76	97
9	5.27	0.17	0.3393	0.0069	0.55459	1887	34	1830	49	103
10	5.23	0.17	0.3348	0.0071	0.50211	1861	34	1832	43	102
11	5.52	0.16	0.3417	0.0072	0.48988	1893	35	1878	30	101
12	5.09	0.14	0.3224	0.0062	0.20318	1801	30	1895	66	95
13	5.04	0.18	0.3162	0.0088	0.54344	1769	43	1904	61	93
14	7.03	0.22	0.368	0.011	0.85838	2016	54	2210	56	91
15	7.85	0.2	0.397	0.012	0.80388	2154	55	2221	67	97
16	11.47	0.26	0.4971	0.0095	0.55	2599	41	2528	49	103

Elliot EN4 - Kyalla Formation										
	Final 207_235	Final 207_235 _Int2SE	Final206_ 238	Final206_238 _Int2SE	Error Correlation _6_38vs7_35	FinalA ge206 _238	FinalAge20 6_238_Int 2SE	FinalAge20 7_206	FinalAge207_2 06_Int2SE	Concordance (%)
1	3.67	0.13	0.267	0.012	0.58213	1525	61	1517	58	101
2	3.67	0.15	0.2683	0.0082	0.63381	1531	42	1553	54	99
3	3.65	0.15	0.275	0.011	0.53699	1562	54	1599	86	98
4	4.02	0.11	0.2778	0.0074	0.76591	1578	37	1620	35	97
5	3.77	0.11	0.2695	0.0076	0.63756	1537	39	1622	43	95
6	3.85	0.15	0.26	0.011	0.76528	1487	56	1631	54	91
7	3.78	0.11	0.2714	0.0074	0.33123	1546	38	1639	60	94
8	4.204	0.094	0.2922	0.0073	0.74654	1651	37	1640	30	101

9	4.44	0.17	0.307	0.012	0.62592	1722	59	1641	57	105
10	4.48	0.12	0.3081	0.0092	0.742	1729	45	1650	35	105
11	4.05	0.11	0.2819	0.0082	0.74801	1604	42	1655	37	97
12	3.95	0.12	0.2852	0.0084	0.64208	1616	42	1657	40	98
13	4.03	0.24	0.272	0.017	0.40034	1549	86	1673	66	93
14	4.42	0.12	0.302	0.008	0.72437	1699	40	1680	36	101
15	4.21	0.13	0.294	0.011	0.85396	1658	53	1680	34	99
16	4.478	0.097	0.3046	0.0073	0.70858	1712	36	1684	30	102
17	4.56	0.13	0.2996	0.0084	0.75409	1693	43	1692	31	100
18	4.22	0.1	0.2965	0.008	0.59543	1676	39	1693	42	99
19	4.23	0.12	0.291	0.011	0.79777	1644	54	1698	41	97
20	3.91	0.13	0.277	0.0071	0.64938	1578	37	1699	50	93
21	4.7	0.12	0.3146	0.0092	0.44302	1768	46	1700	50	104
22	4.13	0.13	0.2848	0.009	0.73447	1614	45	1702	47	95
23	4.4	0.13	0.304	0.011	0.66204	1708	54	1707	51	100
24	4.14	0.12	0.2776	0.0092	0.76815	1578	47	1711	44	92
25	4.58	0.1	0.3099	0.0075	0.8078	1747	37	1714	23	102
26	4.45	0.14	0.301	0.01	0.65117	1696	49	1718	44	99
27	4.55	0.12	0.3026	0.0085	0.46199	1702	42	1720	47	99
28	4.08	0.24	0.281	0.017	0.50537	1592	84	1720	110	93
29	4.43	0.15	0.309	0.011	0.593	1735	53	1722	50	101
30	4.22	0.16	0.282	0.013	0.68419	1601	63	1725	47	93
31	4.37	0.13	0.3006	0.0087	0.67084	1691	43	1732	45	98
32	4.29	0.15	0.289	0.01	0.66926	1641	49	1732	49	95
33	4.63	0.22	0.314	0.012	0.33628	1757	61	1732	79	101
34	4.58	0.19	0.309	0.01	0.47874	1735	51	1737	68	100
35	3.95	0.17	0.285	0.011	0.47147	1612	55	1739	77	93
36	4.29	0.12	0.2942	0.0085	0.71126	1661	42	1741	31	95
37	4.18	0.11	0.2906	0.0076	0.68843	1643	38	1743	37	94

38	4.46	0.13	0.312	0.0092	0.57626	1749	45	1746	43	100
39	4.87	0.13	0.3229	0.0099	0.77496	1809	47	1747	35	104
40	4.724	0.094	0.3173	0.0084	0.71203	1774	41	1747	32	102
41	4.37	0.13	0.299	0.011	0.72221	1685	52	1748	38	96
42	4.33	0.11	0.3039	0.008	0.45037	1708	40	1748	48	98
43	4.45	0.14	0.296	0.018	0.8074	1670	92	1750	70	95
44	4.27	0.12	0.288	0.011	0.62804	1629	55	1751	56	93
45	4.92	0.22	0.314	0.016	0.81487	1759	79	1754	54	100
46	4.54	0.13	0.3107	0.0095	0.70493	1742	47	1755	39	99
47	4.84	0.13	0.3215	0.008	0.63564	1795	39	1757	40	102
48	4.28	0.12	0.286	0.011	0.61025	1618	54	1760	59	92
49	5.1	0.15	0.3234	0.0091	0.64554	1810	45	1761	41	103
50	4.2	0.15	0.284	0.011	0.80073	1608	57	1764	46	91
51	4.6	0.13	0.3167	0.0084	0.48818	1771	41	1767	46	100
52	4.65	0.17	0.316	0.015	0.72076	1767	75	1774	57	100
53	4.32	0.13	0.2969	0.0089	0.58568	1674	44	1775	49	94
54	5.11	0.17	0.33	0.012	0.57979	1835	60	1781	62	103
55	4.83	0.11	0.3121	0.0073	0.46717	1749	36	1784	39	98
56	4.58	0.23	0.303	0.012	0.79287	1703	62	1787	60	95
57	4.68	0.12	0.3203	0.0079	0.53732	1789	38	1787	40	100
58	4.6	0.17	0.3044	0.0088	0.60099	1711	43	1790	56	96
59	5.05	0.13	0.326	0.0079	0.63407	1817	38	1791	43	101
60	4.45	0.2	0.3	0.011	0.58409	1687	53	1793	62	94
61	5.02	0.11	0.324	0.0078	0.62075	1807	38	1795	37	101
62	4.512	0.092	0.304	0.0071	0.60634	1709	35	1798	33	95
63	4.82	0.16	0.311	0.01	0.4517	1742	50	1803	64	97
64	5.22	0.13	0.3277	0.0088	0.44345	1826	43	1806	53	101
65	4.87	0.13	0.3074	0.0094	0.60034	1725	47	1810	48	95
66	4.67	0.1	0.3132	0.0083	0.69371	1754	41	1814	29	97

67	4.73	0.15	0.313	0.011	0.45177	1753	52	1816	60	97
68	4.92	0.14	0.3184	0.0084	0.61062	1785	40	1819	37	98
69	5.29	0.14	0.337	0.01	0.58299	1869	50	1824	48	102
70	5.08	0.13	0.3296	0.0095	0.749	1834	46	1835	34	100
71	5.01	0.14	0.3263	0.0099	0.71708	1817	48	1844	43	99
72	4.66	0.13	0.305	0.011	0.45911	1715	52	1846	57	93
73	5.57	0.17	0.3459	0.0093	0.64968	1913	45	1851	43	103
74	5.15	0.11	0.3308	0.0085	0.70468	1839	41	1861	27	99
75	5.09	0.12	0.3345	0.0084	0.71681	1857	40	1866	31	100
76	4.95	0.14	0.3147	0.009	0.74859	1762	44	1890	36	93
77	5.11	0.1	0.3191	0.008	0.73606	1783	39	1898	30	94
78	5.02	0.17	0.312	0.011	0.6474	1750	53	1898	52	92
79	5.37	0.3	0.337	0.019	0.72102	1870	90	1914	63	98
80	5.53	0.12	0.345	0.0083	0.72234	1908	40	1928	30	99
81	5.77	0.16	0.353	0.01	0.80511	1948	49	1939	30	100
82	6.09	0.3	0.354	0.015	0.59377	1953	70	2073	68	94
83	7.78	0.19	0.396	0.012	0.67251	2148	56	2204	34	97
84	8.39	0.32	0.399	0.015	0.81588	2178	65	2356	34	92
85	9.13	0.25	0.413	0.012	0.62641	2226	53	2367	36	94
86	9.64	0.24	0.442	0.012	0.76041	2371	54	2451	29	97
87	10.44	0.3	0.462	0.013	0.68094	2445	56	2498	38	98
88	10.22	0.22	0.457	0.01	0.63459	2422	46	2500	31	97
89	11.03	0.37	0.478	0.018	0.72622	2522	75	2517	43	100
90	10.56	0.27	0.461	0.015	0.81842	2437	68	2540	32	96
91	15.6	1.1	0.535	0.028	0.679	2760	120	2986	96	92
92	16.61	0.31	0.542	0.013	0.75695	2801	54	2991	24	94

Elliot EN8 - Moroak Sandstone

	Final 207_235	Final 207_235 _Int2SE	Final206_ 238	Final206_238 _Int2SE	Error Correlation _6_38vs7_35	FinalA ge206 _238	FinalAge20 6_238_Int 2SE	FinalAge20 7_206	FinalAge207_2 06_Int2SE	Concordance (%)
1	2.97	0.16	0.232	0.013	0.43688	1341	71	1470	110	91
2	3.38	0.13	0.2601	0.0076	0.39021	1488	39	1475	64	101
3	3.61	0.32	0.277	0.017	0.6433	1575	84	1490	110	106
4	3.22	0.14	0.247	0.01	0.79399	1423	52	1494	44	95
5	3.19	0.12	0.2416	0.0084	0.71655	1401	42	1518	46	92
6	3.467	0.085	0.2641	0.0059	0.37576	1509	30	1519	47	99
7	3.298	0.085	0.2488	0.0073	0.75732	1436	39	1521	38	94
8	3.686	0.095	0.2707	0.0081	0.71045	1547	40	1534	39	101
9	3.64	0.18	0.273	0.011	0.6669	1556	57	1544	76	101
10	3.41	0.21	0.258	0.011	0.78061	1492	64	1545	59	97
11	3.5	0.1	0.27	0.0076	0.68171	1539	39	1547	43	99
12	3.66	0.11	0.2794	0.007	0.74767	1586	35	1550	34	102
13	3.44	0.12	0.2533	0.007	0.73268	1459	37	1559	45	94
14	3.537	0.085	0.2679	0.0062	0.59274	1529	31	1567	42	98
15	3.857	0.087	0.2823	0.0074	0.56882	1606	37	1590	47	101
16	3.62	0.14	0.2675	0.0063	0.28194	1527	32	1593	76	96
17	3.674	0.098	0.2618	0.0088	0.79805	1498	45	1596	44	94
18	3.69	0.13	0.2772	0.0081	0.62924	1576	41	1600	47	99
19	3.68	0.14	0.269	0.011	0.54219	1535	57	1604	57	96
20	3.88	0.11	0.285	0.0073	0.5521	1615	37	1617	41	100
21	3.82	0.1	0.2796	0.0088	0.61624	1587	44	1620	47	98
22	3.73	0.12	0.2772	0.0079	0.54611	1576	40	1626	51	97
23	3.8	0.14	0.277	0.01	0.64246	1574	52	1639	63	96
24	4.08	0.12	0.2887	0.0075	0.45117	1647	37	1640	51	100
25	4.13	0.13	0.2888	0.0087	0.68283	1634	43	1643	41	99

26	3.62	0.14	0.259	0.013	0.7343	1499	69	1647	60	91
27	4.11	0.15	0.289	0.01	0.53266	1633	52	1647	70	99
28	3.98	0.1	0.2861	0.0077	0.78392	1620	39	1659	31	98
29	4.07	0.14	0.2926	0.0087	0.64495	1653	44	1660	49	100
30	4.27	0.11	0.3023	0.0089	0.59934	1701	44	1661	42	102
31	4.4	0.1	0.3153	0.0075	0.64902	1765	37	1665	36	106
32	4.04	0.1	0.2798	0.0079	0.80953	1593	40	1668	29	96
33	4.06	0.14	0.2932	0.0084	0.38478	1655	42	1669	62	99
34	4.44	0.12	0.3027	0.0082	0.63841	1707	40	1669	35	102
35	4.25	0.11	0.3032	0.0085	0.77992	1705	42	1670	32	102
36	4	0.15	0.282	0.011	0.80685	1602	54	1674	35	96
37	4.45	0.17	0.305	0.01	0.88573	1719	53	1681	33	102
38	3.93	0.12	0.2797	0.0097	0.80432	1587	49	1687	36	94
39	3.88	0.11	0.2763	0.0086	0.53284	1577	42	1688	48	93
40	4.34	0.14	0.3	0.012	0.74626	1702	60	1689	48	101
41	4.37	0.11	0.3034	0.0075	0.78187	1706	37	1689	30	101
42	4.5	0.11	0.3066	0.0084	0.70076	1731	41	1698	36	102
43	4.25	0.17	0.294	0.018	0.80102	1660	89	1701	60	98
44	4.37	0.1	0.3006	0.0084	0.7292	1692	42	1708	35	99
45	3.96	0.16	0.279	0.01	0.54262	1584	51	1718	60	92
46	4.46	0.14	0.2975	0.0093	0.60625	1676	46	1719	48	97
47	4.33	0.11	0.303	0.0079	0.62597	1704	39	1720	38	99
48	4.22	0.15	0.294	0.013	0.76858	1672	61	1723	37	97
49	4.54	0.11	0.3047	0.0079	0.63491	1712	39	1724	36	99
50	4.37	0.13	0.3047	0.0082	0.51585	1712	41	1730	51	99
51	4.18	0.11	0.2883	0.0075	0.64115	1631	37	1732	39	94
52	4.18	0.11	0.2875	0.008	0.62712	1628	40	1743	41	93
53	4.38	0.15	0.3	0.01	0.31994	1705	52	1749	79	97
54	4.595	0.097	0.3145	0.008	0.62364	1760	39	1761	34	100

55	4.68	0.15	0.316	0.01	0.69658	1766	52	1772	42	100
56	4.84	0.11	0.3174	0.0082	0.78579	1781	39	1782	28	100
57	5.15	0.14	0.336	0.01	0.6643	1867	50	1792	40	104
58	4.62	0.16	0.3015	0.0091	0.75342	1704	46	1812	39	94
59	8.4	0.23	0.412	0.013	0.64511	2221	61	2334	37	95
60	9.97	0.24	0.458	0.013	0.83437	2436	60	2442	26	100
61	10.19	0.27	0.457	0.012	0.73477	2421	54	2457	32	99
62	18.19	0.45	0.569	0.015	0.66012	2902	62	3049	32	95

	Elliot E18 - Moroak Sandstone									
	Final 207_235	Final 207_235 _Int2SE	Final206_ 238	Final206_238 _Int2SE	Error Correlation _6_38vs7_35	FinalA ge206 _238	FinalAge20 6_238_Int 2SE	FinalAge20 7_206	FinalAge207_2 06_Int2SE	Concordance (%)
1	2.9	0.35	0.233	0.025	0.73096	1350	130	1422	91	95
2	3.78	0.1	0.2791	0.0093	0.74404	1585	47	1626	39	97
3	3.72	0.15	0.2635	0.0091	0.70495	1506	47	1642	51	92
4	3.79	0.12	0.2667	0.0071	0.64247	1523	36	1647	42	92
5	4.08	0.17	0.291	0.013	0.74501	1647	64	1650	56	100
6	3.78	0.14	0.27	0.011	0.73693	1541	54	1655	41	93
7	4.2	0.3	0.292	0.013	0.18509	1665	69	1660	140	100
8	4.021	0.089	0.2826	0.0054	0.62515	1604	27	1662	34	97
9	3.92	0.14	0.2733	0.0096	0.67933	1556	49	1667	47	93
10	3.98	0.12	0.2831	0.0086	0.55006	1604	43	1684	49	95
11	4.179	0.082	0.2897	0.0066	0.56233	1638	33	1694	34	97
12	4.48	0.29	0.3	0.012	0.238	1690	61	1700	110	99
13	3.94	0.16	0.2791	0.009	0.77939	1600	48	1706	48	94
14	4.03	0.16	0.278	0.013	0.6915	1581	68	1712	47	92

15	4.45	0.14	0.2943	0.0081	0.33816	1661	40	1734	53	96
16	4.67	0.11	0.3102	0.0083	0.60389	1739	41	1756	43	99
17	4.5	0.13	0.296	0.0089	0.7104	1669	44	1761	42	95
18	4.66	0.16	0.3076	0.0099	0.31054	1732	48	1782	65	97
19	4.51	0.1	0.293	0.007	0.7406	1655	35	1795	28	92
20	4.99	0.13	0.312	0.012	0.74985	1751	60	1915	48	91
21	5.41	0.19	0.33	0.012	0.65201	1834	58	1925	53	95
22	5.55	0.16	0.33	0.011	0.81487	1844	52	1960	34	94